Temple University

College of Engineering

Bioengineering

Preliminary Design
Dimensions and type of bioreactor used (not updated)

Partial Gravity Bioreactor

Presented By: Team #13

Dmitry M Hackel *Irene Bui*

Jake Fisher *Zenub Abouzid*

Supervised By:

Dr. Yah-el Har-el & Dr. Peter Lelkes

0 9 – 2 1 – 2 0 2 5

Acknowledgment

We want to extend our most profound appreciation to the following individuals and organizations who have contributed to the completion of this project:

- Dr. Yar-el Har-el, for providing guidance and feedback throughout the course of this project through her professor and advisor roles.

- Dr. Peter Lelkes, a subject matter expert and our advisor, for providing valuable information and resources for our research.

- Dr. Jonathan Gerstenhaber, for providing valuable information, previous prototypes, and ideas that paved the way for the prototype.

- Brian Amin and Matthew Short, a previous team who completed a similar topic, for giving us the time to explain their prototype in more depth.

- Temple University, for providing access to their machines, labs, and space.

Additionally, we would like to express our gratitude to all those who have supported us in ways both seen and unseen. Without your contributions and presence, this project would not have been possible.

Thank you.

Abstract

The progress of human exploration to space, the Moon, and Mars is not considered safe because of the limited understanding of how partial gravity impacts human cells. This issue has not been fully addressed due to cost limitations and the difficulty of accurately simulating partial gravity on Earth. This project focused on developing a validated prototype for a partial gravity bioreactor. By successfully simulating the mathematical model and conducting tests to validate the prototype visually, the accuracy between the models can be determined.

Table of Contents

List of Acronyms/Abbreviations

MOND	Modified Newtonian Dynamics
ACME	Advanced Combustion via Microgravity Experiments
NASA	The National Aeronautics and Space Administration
ISS	International Space Station
$0G$	Zero Gravity
μG	Microgravity
$\frac{1}{6}G$	Lunar Gravity
$\frac{3}{8}G$	Martian Gravity
$1G$	Earth Gravity
RWV	Rotating Wall Vessel
UNSDG	United Nations Sustainable Development Goals
SDG	Sustainable Development Goals
DGD	Degree of Gravity Dispersion
RGP	Reduced Gravity Paradigm
STLV	Slow-Turning Lateral Vessel
HARV	High Aspect Ratio Vessel
MAGICIAN	Mars Artificial Gravity Habitat with Centrifugation

List of Figures

List of Tables

1. Problem Statement

1.1 Overall Objective

Since the 1960s, space exploration has yielded intriguing discoveries that continue to unfold over time. Yuri Gagarin became the first human in space in 1961, paving the way for thousands of astronauts and cosmonauts to follow him as the years passed [1]. Various theories have been proposed based on space, including the Croatian Barrel Theory, which explains how the solar system, stars, and other celestial bodies formed [2][3]. In 2002, research refuted the theory that gravity alone governs the universe, as it could not explain specific astronomical observations [4]. Sanders and McGaugh modified Newtonian gravity as an alternative to cosmic dark matter, known as Modified Newtonian Dynamics (MOND), correlating a relationship between the acceleration from Newtonian gravity and the observed acceleration at any radius in a galaxy [5][6].

Exploring space not only reveals discoveries beyond our planet, but it also uncovers truths that enhance and govern our lives. Advanced Combustion via Microgravity Experiments (ACME) investigates fuel efficiency and pollutant production in combustion under microgravity conditions on Earth [7]. One of their investigations, Flame Design, studied the quantity of soot produced under different flame conditions [7]. Such a discovery could lead to more efficient combustion, reducing pollution on Earth [7]. In the ongoing Moon exploration, researchers found that the Moon's gravity affects Earth's tides, plant growth, animal behavior, and agricultural practices [8]. Moreover, models have shown that the Earth-Moon coupled magnetospheres provide a buffer against the solar wind, allowing for a reduction in Earth's atmospheric loss to space [9]. The National Aeronautics and Space Administration (NASA) has been exploring Mars for over sixty years to decide whether it is or was a habitable world [10]. Since Mars is the most similar planet to Earth in the Solar System, understanding its surface and evolution is crucial for preparing for future human exploration [11]. With evidence suggesting that Mars was once full of water, warmer, and had a thicker atmosphere, it is highly likely that Mars could be a habitable environment [11].

Traveling beyond Earth's atmosphere to investigate potential extraterrestrial life entails considerable risks and substantial financial investment. Considering that human physiology is heavily dependent on gravity, any significant fluctuations in gravitational force may lead to serious health issues [12]. Gravity, as a vector quantity, influences all objects by determining their weight relative to their mass [13]. Biological organisms respond to environmental stimuli—including gravity—by developing unique morphological traits, physiological characteristics, behaviors, and habitat preferences [13]. The sensitivity of organisms to changes in gravity increases with their size and mass, with single cells enduring exposures up to 10^5G and humans tolerating gravitational forces of 4-5G [13]. At the cellular level, cells comprise organelles, each with mass and thus subject to gravitational forces [14]. Variations in gravitational vectors could disrupt cellular homeostasis, affecting structural integrity, composition, and orientation, such as the cytoskeleton, which maintains cellular shape [14]. Additionally, numerous studies have documented genes exhibiting sensitivity to gravity alterations, including modifications in cytoskeletal gene expression pathways and gene inhibition following microgravity exposure [15][16]. In the absence of gravity, cellular growth pathways shift, and metabolic processes adapt due to changes in reactive oxygen species levels [17][18]. Furthermore,

cellular adaptation to gravity is vital for tissue adaptation, with bones containing osteocytes that sense and respond to varying gravitational loads [13].

Such cellular changes impact the entire human system. Astronauts exposed to microgravity undergo physiological deconditioning in systems sensitive to mechanical loading, including the cardiovascular, pulmonary, and musculoskeletal systems [19]. To mitigate these effects, International Space Station (ISS) crew members engage in rigorous exercise; however, despite extensive physical activity, astronauts still return from their six-month ISS missions exhibiting decreased calf muscle volume and strength, loss of bone mineral density, and reduced peak oxygen uptake [20][21][22][23].

Given that, it is highly unethical to send people into space without understanding the effects of gravitational changes on the body. This paper discusses a validated proposed prototype of a device that cultures cells under the influence of partial gravity and microgravity, enabling the correlation of specific cell behaviors with gravitational differences.

1.2 Background

Understanding the effects of partial gravity on humans is less extensively studied due to the high costs associated with conducting tests in partial or microgravity environments. Between 1960 and 1973, the research experience and studies gained during the Apollo missions—focused on lunar exploration—provided valuable insights into the diverse effects of partial gravity on the human musculoskeletal, cardiovascular, and respiratory systems, employing either microgravity or Earth's gravity as controls [24][25]. However, the Apollo missions cost approximately $25.4 billion in 1969, equivalent to roughly $217 billion in 2024 [26]. Following these missions, despite the lack of subsequent lunar landings, the failures in early missions facilitated advancements in spacecraft design, including the incorporation of additional protective layers and the development of new, safer materials, alongside the integration of computer systems for troubleshooting purposes [27]. In 2019, the health impacts of a year-long space mission were examined at the molecular and psychological levels by comparing the DNA sequences of twin brothers—Mark and Scott Kelly—with Mark Kelly remaining on Earth, serving as the control, and Scott Kelly participating in spaceflight [28][29]. The study revealed that extensive multisystem and gene expression changes occur during spaceflight [28]. Astronauts may face risks including mitochondrial dysfunction, immunological stress, vascular modifications, fluid shifts, and cognitive performance decline, along with alterations in telomere length, gene regulation, and genome integrity [28].

Given the expenses and decommissioning of the ISS, researchers endeavored to replicate partial gravity conditions on Earth, such as employing a pulley-spring system to simulate partial gravity for rodents (refer to Figure 1) [23][30]. However, a limitation of the apparatus was that only the tail was suspended rather than the entire body, resulting in a weight shift within the rodent's body and thus failing to provide a truly accurate simulation [30].

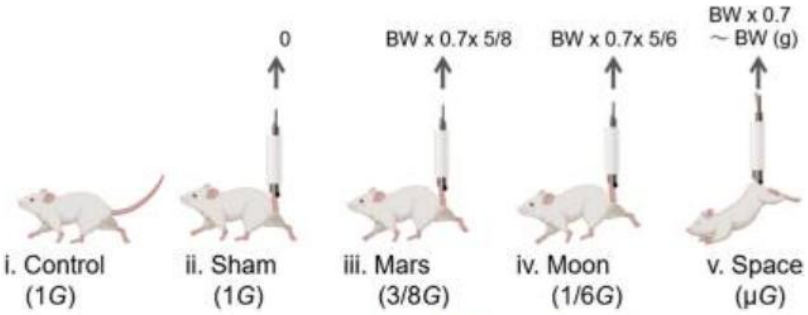

Figure 1. Experimental Design for Simulated Partial Gravity Apparatus for Rats
The figure shows the groups of experimental rats with the Control group ($1G$) (i); the sham group with SA ($1G$) (ii); the Mars group ($\frac{3}{8}G$) (iii); the Moon group ($\frac{1}{6}G$) (iv); and the interplanetary space (μG) group (v) [18].

The effects of gravity on an object may manifest as either displacement or deformation [31]. Microgravity creates distinctive environments conducive to cell growth, whereas partial gravity (such as on the Moon and Mars) may yield markedly different effects [32]. To comprehensively understand the concepts related to partial gravity apparatuses, it is imperative to distinguish between zero gravity, gravity, microgravity, and partial gravity. Gravity is an abstract phenomenon that can be quantified; however, its fundamental cause remains unknown [33]. The gravitational constant is not a force or acceleration but is employed as a scaling factor in Newton's Law of Gravitation, as demonstrated in Eq. 1[33][34].

$$F = \frac{Gm_1m_2}{r^2} \quad (1)$$

Equation 1. Gravitational Force Equation

Where:
F = gravitational force
m_1 = mass 1
m_2 = angle between the inclined plane and the base
r = distance between masses
G = universal constant ($6.67384 * 10^{-11}\ \frac{m^3}{\frac{s^2}{kg}}$)

Zero gravity ($0G$) describes a condition where there is an absence of gravitational force exerted on an object, which occurs either due to its infinite distance from any other gravitational body or when the net sum of all forces acting upon it equals zero [35]. Microgravity (μG) pertains to a state in which the net gravitational force exerted on an object is minimal, typically within the range of 10^{-4} to $10^{-6}G$ [36]. Although the object remains influenced by gravitational forces, it undergoes continuous free fall [36]. This perpetual free fall occurs when the object falls at a constant velocity but does not contact a surface [36]. As a result, the difference between the initial and final velocities manifests as a constant acceleration (g) [36]. Partial gravity refers to a gravitational force that is diminished but not absent compared to Earth's gravitational acceleration, such as on the Moon, where gravity is approximately $\frac{1}{6}G$, on Mars $\frac{3}{8}G$, and on

Earth $1G$ [29]. On Earth, the simulation of partial gravity can be achieved through techniques such as centrifugation, parabolic flight, or modified rotation devices that generate acceleration less than $1g$ [37].

To investigate gravitational effects, cell culturing is regarded as the most efficacious method, with bioreactors serving as the optimal apparatus, given their ability to supply controlled nutrients and biomimetic stimuli for cellular growth [38]. A bioreactor is defined as a vessel in which a chemical process involving organisms or biochemically active substances derived from such organisms is conducted, or a system designed for cell cultivation, first developed in 1964 (refer to Figure 2) [39].

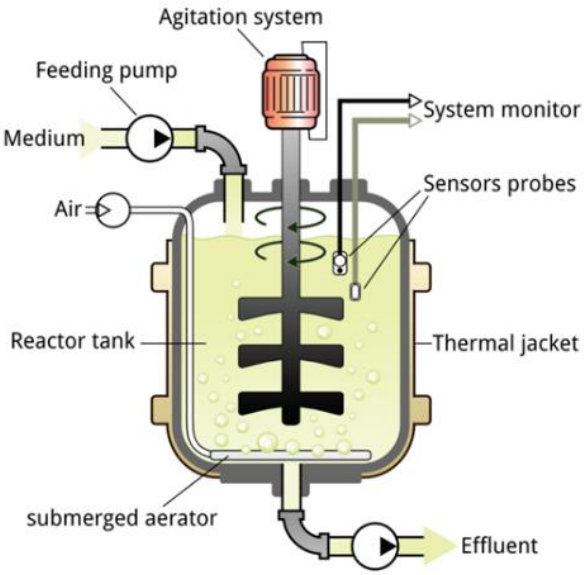

Figure 2. Basic Bioreactor
The figure shows the basic bioreactor components. It includes a feeding pump, air, medium, agitation system, reactor tank, and other elements to ensure an automated culturing system [39].

Previous bioreactors were designed as ground-based systems to mimic aspects of weightlessness or reduced gravity experienced by biological organisms in space. Recognizing this potential, in the mid-1980s, NASA researchers at Johnson Space Center needed to develop a way to study the effects of microgravity on human tissues as the shuttle fleet was grounded after the Challenger disaster [40]. They invented a rotating bioreactor to address the challenge of treating injured astronauts in space and to simulate weightlessness on Earth [40]. In μG, the bioreactor allows cells to grow in three-dimensional tissue structures that closely resemble natural development, aiding advances in medicine both on Earth and in space [40]. In 2002, Houston-based Regenetech Inc. licensed NASA bioreactor technology and patents that can expand adult stem cells (from blood to bone marrow) by 50-200 times in less than a week, providing safer, faster, and more affordable cell sources for therapies [40].

Partial gravity bioreactors, although not extensively studied, have been previously examined. Research dating back to the 1900s has investigated the effects of clinostats, or rotating wall vessels, on biological samples [41]. Clinostats were invented by Julius Sachs, who rotated growing plants around their growth axis [41]. These devices exist in one-dimensional (1-D) or two-dimensional (2-D) forms, depending on the

dimensions of the rotated axial line or the entire experimental area [42]. Subsequently, enhancements to the clinostat with two axes led to the development of three-dimensional (3-D) clinostats, known as the Random Positioning Machine (RPM) (refer to Figure 3) [42][43].

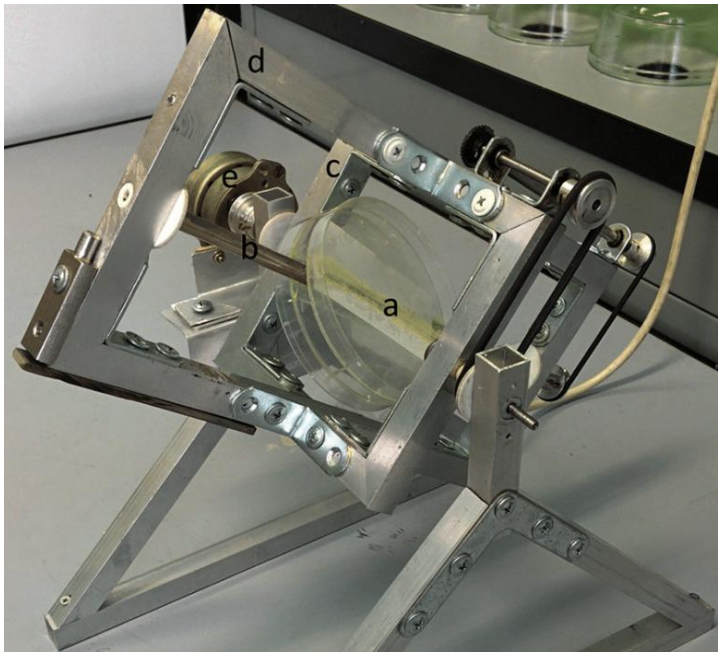

Figure 3. 3D Clinostat

The figure depicts a three-dimensional clinostat employed to investigate the effects of microgravity on seed germination: a, insert for Petri dishes; b, rotating shaft; c, inner frame; d, outer rotating frame; e, motor [43].

Numerous early-stage partial gravity bioreactors have been investigated using plant species capable of continuous growth under Earth's gravitational forces [44]. Initial implementations included clinostats, which maintain a constant rotation of a sample to effectively average the gravitational vector to near zero [41]. This form of a partial gravity bioreactor does not fully replicate “true” microgravity, as cells continue to experience mechanical stimulation and gradients that differ from actual microgravity conditions [41]. Subsequently, rotating wall vessel (RWV) bioreactors were introduced as a specialized variant of clinostats [41]. RWVs are fluid-filled cylinders containing cells, designed to create a low-shear, controlled environment conducive to cellular differentiation in three-dimensional space [45]. By rotating at a terminal velocity, RWVs facilitate proper nutrient delivery to the tissue culture, thus promoting healthy tissue and cell growth [45]. In 2018, a previous senior design team utilized the stability of RWVs for cell culturing while incorporating the partial gravity factor using an inclined plane to partially cancel the gravitational vector, allowing cells to experience a form of partial gravity (refer to Figure 4).

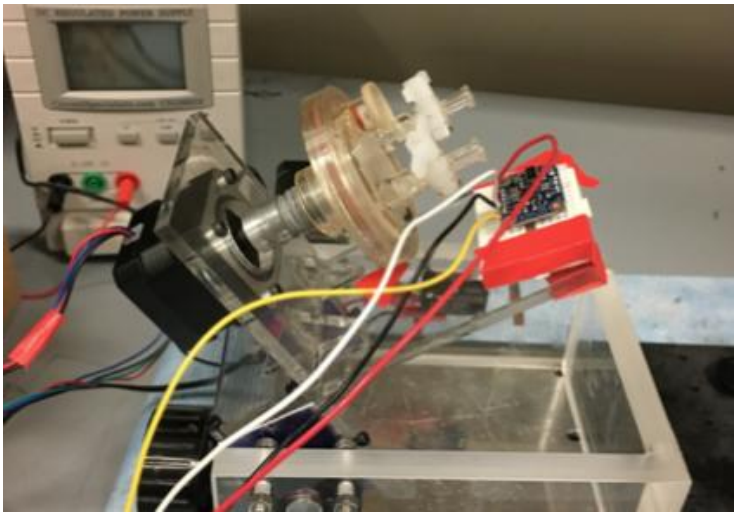

Figure 4. Partial Gravity Bioreactor
The figure depicts the prototype of a partial gravity bioreactor, designed by an earlier senior design team. It comprises a Rotating Wall Vessel (RWV) affixed to an inclined plane that simulates partial gravity.

1.3 Needs Statement

Building a partial gravity cell culturing prototype would enable the study of the relationship between cell properties and different gravitational environments, therefore allowing for correlation between gravitational differences and cell properties.

1.4 Implications of Project Success

In the event of the prototype's success, both terrestrial and extraterrestrial life would benefit significantly. Comprehending the effects of varying gravitational conditions on cellular behavior would facilitate more precise conclusions regarding human space exploration. Such findings would underpin the development of solutions aimed at safeguarding human safety beyond Earth. Facilitating human travel to outer space, including destinations such as Mars and the Moon, enhances our knowledge of extraterrestrial regions and addresses fundamental questions concerning alien life forms. Additionally, this research has the potential to identify new planets or locations in space where humans might establish a new life.

The success of the prototype closely correlates with several United Nations Sustainable Development Goals (UNSDGs) [46]. SDG 3: Good Health and Well-being is supported, as the device facilitates controlled studies on how partial gravity influences cellular development, physiology, and long-term health in space [47]. By understanding these effects, the prototype can inform the design of countermeasures, treatments, and potentially therapeutic approaches for conditions such as bone loss and muscle atrophy, which are of critical concern for astronauts [28]. Accordingly, the prototype would contribute to ensuring healthy lives for humans [47]. Furthermore, the prototype advances SDG 12: Responsible Consumption and Production through the implementation of a closed-loop biological system, an approach essential for

sustainable space habitats and beneficial for the efficient utilization of resources on Earth [48]. The use of a bioreactor enhances system control in cultivating cells, enabling accurate, real-time monitoring, early problem detection, reproducibility, and cost efficiency [49]. In this context, SDG 13: Climate Action is addressed by demonstrating how biological systems adapt to extreme and changing environments, thereby informing strategies for ecosystems on Earth [50]. Lastly, SDG 9: Industry, Innovation, and Infrastructure is pertinent, as the development of the prototype signifies an innovative research platform that represents the convergence of biotechnology and space technology [51].

2. Design Criteria

To guarantee the feasibility of the prototype, the design criteria are classified as either non-negotiable (mandatory) (refer to Table 1) or negotiable (desirable) (refer to Table 2). However, owing to the complexity of the project, these criteria are divided into two primary domains: partial gravity and the prototype.

2.1 Non-Negotiable Criteria

Four criteria must be satisfied to deem the partial gravity component in the project successful: gravitational type, simulation, visual validation, and movement.

Gravitational Type: With NASA deorbiting the ISS, the ability to conduct experiments in the unique microgravity laboratories would be impossible [52]. Therefore, gravitational experiments conducted on Earth should encompass the primary missions previously planned. According to NASA, traveling to the lunar surface and around the Moon would facilitate scientific discoveries that prepare humans for subsequent exploration, including Mars [53]. As the Moon and Earth represent the two most significant gravitational environments, lunar gravity ($\frac{1}{6}G$) and Martian gravity ($\frac{3}{8}G$) warrant careful consideration [54]. To obtain more accurate data, Earth's gravity ($1G$) and microgravity (μG) should also be included to ensure that the same cells are subjected to all gravity levels and to serve as references for previous experiments [54][55].

Movement: To cultivate cells effectively, the partial gravity method should not present any issues for cell culture practices. Given the high sensitivity of cells to their environment, the technique employed to simulate partial gravity must prevent excessive vibrations or inconsistent cell motion [56]. To accomplish this, the procedure for attaining different gravitational levels should function smoothly, enable cells to undergo free fall, and simultaneously minimize shear stress on the cells, maintaining these conditions continuously.

Simulation: The partial gravity effect on cells has not yet been observed or tested. However, visualizing gravity is not applicable, since gravity is a theory [57]. Utilizing mathematics, fluid mechanics, and particle mechanics, a mathematical model should be developed for partial gravity.

Validation: Since models are simplified representations of the systems studied, models, to a degree, are all incorrect at least in some details [58]. Therefore, visualizing the specimen would provide further insight into the accuracy of the model and constitutes a form of validation. It is necessary to visualize the specimen under different gravitational levels to ensure the model's accuracy.

Three criteria should be met to consider the prototype successful: size, material, and specimen culturing stability.

Size: Since the prototype's placement may be limited to the incubator, its overall dimensions are also constrained. The Nuaire NU-5810E incubator is considered the most suitable and effective location based on previous designs because it operates at 37°C with 98% humidity [59]. The maximum size of the prototype is limited by the incubator's internal capacity, which measures $21 \times 20 \times 20.8\ in$.

Material: Given the potential placement of the prototype within an incubator, the selected materials must endure both room temperature and 37°C, in addition to 98% humidity [59]. Furthermore, the prototype is anticipated to maintain stability for at least four months.

Stability of the Specimen Culturing Component: Considering that the prototype integrates the cell culturing component and motion system responsible for partial gravity simulation, it is imperative that the attachment of the cell culturing component to the prototype's framework is secure to ensure precise results, given the sensitivity of cells to their environment [56]. Throughout any movement induced by the partial gravity simulation, the cell culturing section must remain stable; that is, it should neither wobble nor detach.

Table 1. Non-Negotiable Needs

Priority	Requirement	Metric	Target Values/ Range or Pass/Fail	Justification
Non-negotiable	Gravitational Type	Partial Gravity and Controls	Range: μG to $1G$ Lunar gravity ($\frac{1}{6}G$) Martian gravity ($\frac{3}{8}G$) Earth's gravity ($1G$) Microgravity (μG) [54][55]	NASA's Goals [53]
Non-negotiable	Partial Gravity Movement Causes Steady Flow	Partial Gravity Accuracy	Pass/ Fail Using Model and Visuals	Inaccuracy of data due to cell sensitivity [56]
Non-negotiable	Simulation	Mathematical Model	Pass/ Fail	Accuracy and Validation
Non-negotiable	Validation	Visual	Pass/ Fail	Accuracy and Validation of Model [58]
Non-negotiable	Size	Dimensions	$21 \times 20 \times 20.8\ in$	Nuaire NU-5810E Incubator Restricted Area [65]
Non-negotiable	Material	Strength and Durability	Pass/ Fail to withstand room temperature and 37°C, along with 98% humidity [59]	Project Duration
Non-negotiable	Cell Culturing Component Stability	Stability	Pass/ Fail of component wobbling/detachment	Inaccuracy of data due to cell sensitivity [56]

The table delineates the seven non-negotiable criteria essential for the validation of the prototype. Regarding partial gravity, the requirements encompass gravitational type, simulation, partial gravity movement, and verification processes. Concerning the prototype, the criteria related to the base and partial gravity—such as size, material, and the stability of cell culturing components—are considered fundamental. Additionally, the metric, target range, and justification for each criterion are systematically provided.

2.2 Negotiable Criteria

Regarding the negotiable criteria, four factors have the potential to enhance the prototype if they are duly implemented. Firstly, the integration of an automated imaging system for cellular analysis would enable users to evaluate the cell culture comprehensively and acquire more profound insights into cellular interactions across various temporal stages. Secondly, the advancement of mathematical models into computational simulations would facilitate a more detailed understanding of the fluid dynamics affecting the cells. Thirdly, incorporating a broader spectrum of gravitational conditions would allow for a more precise simulation of human body movements, from Earth to extraterrestrial environments. Lastly, cultivating the cells would ensure that the prototype is suitable for cell culturing, with a cell viability exceeding 80%, in accordance with ASTM F2739-19 [60][61].

Table 2. Negotiable Needs

Priority	Requirement	Metric	Target Values/ Range or Pass/Fail	Justification
Negotiable	Automated Imaging System	Data Tracking	> 30 FPS	To record the cell's activity during culturing
Negotiable	Computational Models	Modeling Accuracy	Pass/ Fail	To have a more sophisticated model for partial gravity
Negotiable	Broader Range of Gravitation	Partial Gravity and Controls	More than four partial gravities achieved	To include minimal gravitational changes during spaceflight
Negotiable	Cell Culturing	Validation	Cell Viability >80% [60]	ASTM F2739-19 [61]

The table delineates the four negotiable criteria for the enhancement of the prototype. These criteria encompass an automated imaging system, the development of computational models, an expanded gravitational environment, and cell culturing. The table supplies the metric, target range, and justification for each criterion.

3. Solutions

The project concentrates on validating partial gravity, which involves ensuring that the tested specimen experiences the intended gravitational force. Cell culturing methodologies will not be addressed. To eliminate any effects attributable to cell culturing, the same culturing component will be employed across all proposed solutions.

3.1 Bioreactor Solutions

Bioreactors are the predominant method utilized in cell cultivation due to their capability to sustain biologically active environments and to regulate parameters such as pH, temperature, oxygen tension, media perfusion rate, as well as their capacity to apply external stimuli [62]. Various types of bioreactors exist, including wave motion, stirred tank, and rotating wall vessels (refer to Supplementary Table S1) [63]. Since cells are susceptible to mechanical stresses such as shear forces and microfluidic flow, which may result in cellular structural failure and reduced viability, the selection of a bioreactor should be based on its ability to exert minimal shear stress on the cells [64]. Cells cultured in microgravity and ground-based microgravity analogs present a low-shear stress environment suitable for cell cultivation [65]. Rotating wall vessels (RWVs) are effective at small volumes (<10L) and can simulate microgravity with low turbulence and minimal impact [63].

Given the same bioreactor employed for cell cultivation, two potential choices of the RWV used are examined. The solutions are based solely on the RWV's bubble issue.

Solution R.A: Standard Bioreactor

RWVs have been observed extensively to provide continuous sedimentation of particles through a culture medium [66]. The rotation provided by the RWV is special since it induces minimal cellular shear and turbulence [66]. Figure 5 shows the side view of a rotating wall vessel [67].

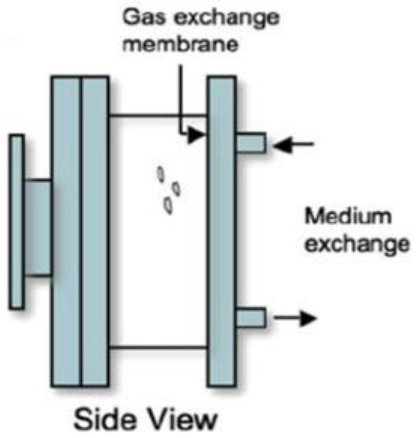

Figure 5. Schematic Side View of Rotating Wall Vessel Bioreactor

The rotation facilitates the complete immersion of the particle seeded in the medium. Consequently, utilizing the standard RWV contributes to the advancement of knowledge in cell culturing. RWV systems have demonstrated success in cultivating prostate organoids, liver tissue, colon carcinoma, cartilage, and many other cell types [67].

Solution R.B: Bubble Trapping Bioreactor

One of the complications when it comes to RWVs is the bubble formation during operation [68]. The formation of bubbles interferes with the RWV environment, including as zero headspace, low-shear, and simulated microgravity [68]. Laminar flow needs to be developed so that the liquid within the bioreactor acts as a rotating object, a novel bubble capture HARV design would reduce and potentially remove the common issues of bubble formation while also reduce operational media volume without reducing radius.

The bioreactor is designed with a hollow microporous plastic tube and an exit channel to catch bubbles. It is approximately 15 cm long to ensure proper perfusion through the microporous plastic (seen in Figure 6). The small hollow tube made of sponge-like plastic with tiny pores has a plug placed partway down its length. When media is pushed down the tube, an exchange of old and new media occurs, providing nutrients to the circulating cells. This unique design allows for the input of filling to go straight into the main bioreactor chamber, which is then outputted through the channel that catches bubbles and allows for the exchange of used up media (see Figure 7) [69][70].

Although this design of bioreactor is more optimal, it is only if the bioreactor is built and proven to not sustain any major issues during construction within the short time for this project. Many small mistakes with the design of this system could eliminate the fragile environment needed to develop an RWV and cell culture environment.

Furthermore, bubbles or flow disruptions do not simply represent mechanical inefficiencies; they directly impact the ability of cells to remain in suspension, receive nutrients, and oxygen delivery. The presence of bubbles can also increase the shear forces impacted on the cells.

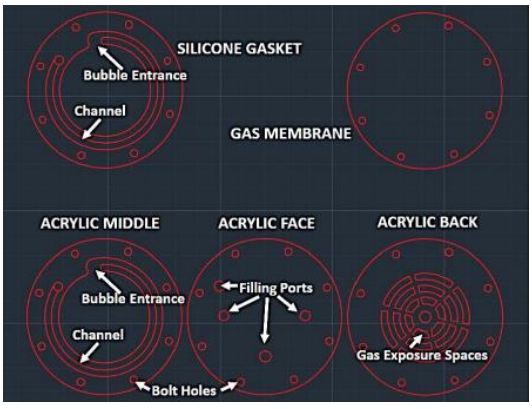

Figure 6. Design of Bioreactor

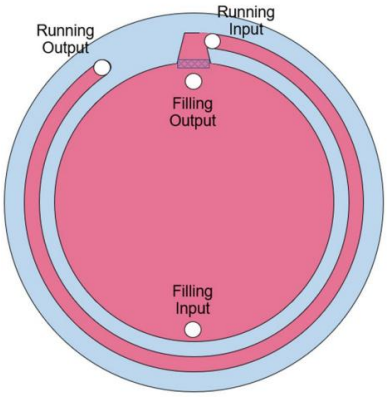

Figure 7. Bubble Trapping Bioreactor Sketch

3.2 Partial Gravity Solutions

As for partial gravity, three potential solutions for addressing partial gravity are examined.

Solution P.A: Inclined Plane (Dual Motors)

The proposed solution entails the enhancement of an existing design through the development of the partial gravity prototype using an RWV on an inclined plane, equipped with a dual-motor system (refer to Figure 8) The use of the inclined plane was previously studied and found to be a successful simulation of lunar gravity [71]. The design consists of three components: a foundational structure, a component that securely holds the bioreactor along with the motor responsible for generating rotational force, and a final system designed to adjust the angle of the motor and bioreactor to simulate partial gravity.

The base will be constructed as a rectangular structure capable of supporting the bioreactor assembly with stability and durability. The main section of the RWV will include a motor attached to the bioreactor to enable rotation, and this assembly will be mounted to the system that adjusts the bioreactor's angle. Next, a camera will be mounted on the same part of the device to accurately simulate the bioreactor's angle and allow monitoring of the cells during their rotation within the RWV. For the final part, a secondary motor capable of adjusting to various angles will be used, and it will have an attachment to the bioreactor system. The secondary motor should be able to set angle variations at least at four different positions to mimic the following gravitational conditions: $1G, \frac{3}{8}G, \frac{1}{6}G$, and μG. The rough sketch of the proposed solution is seen in Figure 9.

These improvements to the current designs enhance the ability to validate the actual generation of partial gravities. The addition of a camera will enable real-time, accurate observation of cell reactions. Furthermore, this design provides a means for validation through modeling and mathematical analysis to confirm that this configuration produces the desired partial gravity effect for RWV.

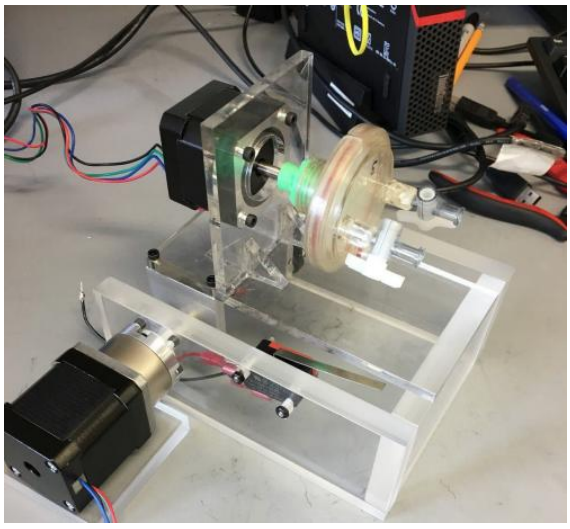

Figure 8. Inclined Plane Bioreactor with Dual Motors

The figure depicts the inclined plane bioreactor, designed by the previous senior design team. Utilizing two motors and an inclined plane, the previous team simulated partial gravity.

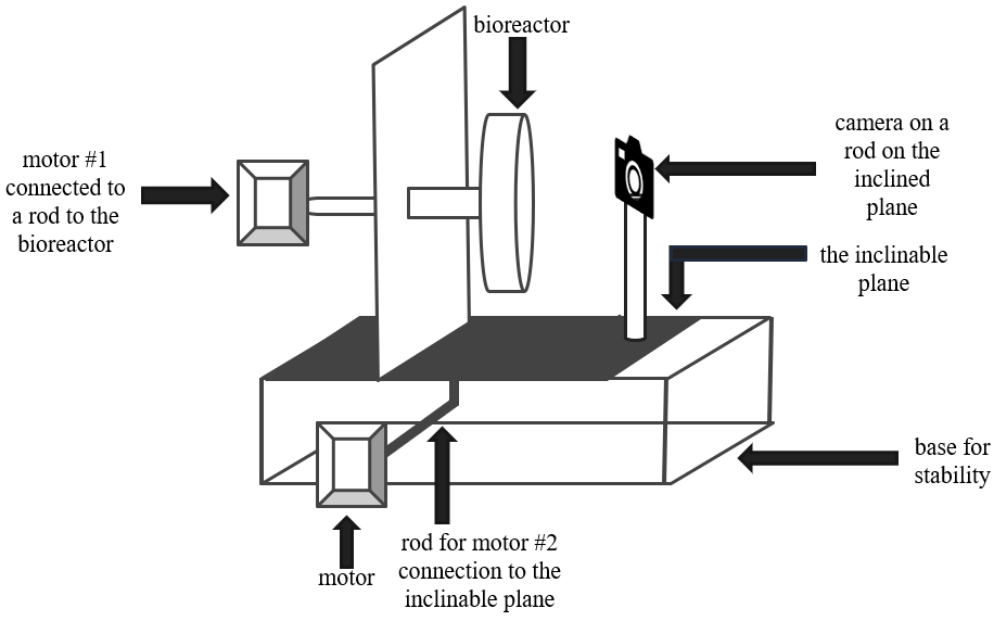

Figure 9. Rough Sketch of Inclined Plane with Dual Motors

The figure illustrates the preliminary sketch of the inclined plane setup with dual motors. The bioreactor is affixed to one motor, while the inclined plane is connected to another motor. The camera is positioned parallel to the bioreactor to ensure that the entire view of the bioreactor is captured.

Solution P.B: Four Centrifugations

The proposed solution concentrates on the centrifugation concept to emulate partial gravity on biological cells. The rationale for employing centrifugation is that the centrifugal force will generate an apparent gravity during rotational motion [72]. In fact, a proposed 0.16G acceleration was achieved by connecting two modules via a 300-meter tether and rotating them at 1 rpm [72]. O'Neill's 1.8 km radius Stanford torus, spinning at 1 rpm, produced Earth's gravity in space [72]. However, in numerous other examples and proposed solutions, the relationship between rotation and radius is closely interdependent. The centripetal acceleration is inversely related when tangential velocity remains constant, but has a direct relationship when angular velocity remains constant [73]. Consequently, centrifugation is a valid method to generate partial gravity, which can be as low as 0.001G [74]. However, during centrifugation, it is crucial to rotate the system around its own axis to ensure no sedimentation takes place, as seen in Figure 10 [75].

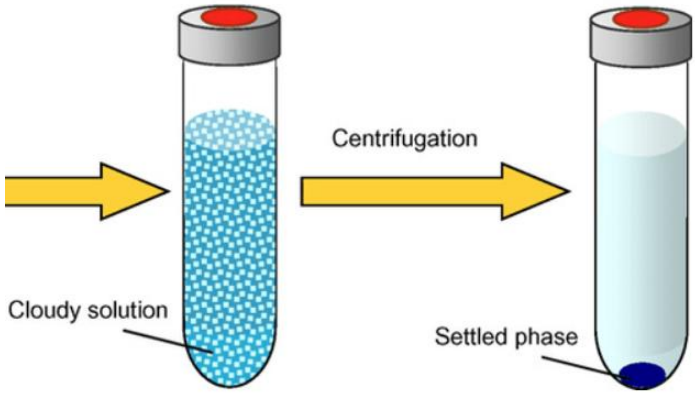

Figure 10. Schematic Diagram of Centrifugation to Settle Particles

The proposed solution emphasizes the capability to utilize a set of rotating bioreactors tailored for specific gravitational forces. As the system encompasses four distinct gravity levels, the solution entails four separate bioreactors, each stabilized by circumferential holes. These bioreactors would feature varying radii, enabling the simulation of partial gravity without subjecting the cells to undue shear stress from rotational motion and friction within the medium. Additionally, each bioreactor would be equipped with its own motor. Regarding the observational equipment, a camera will be positioned to provide a frontal view of all bioreactor surfaces, extending from the base of the prototype in an L-shaped configuration to encompass all units. Figure 11 illustrates the overall schematic of the design.

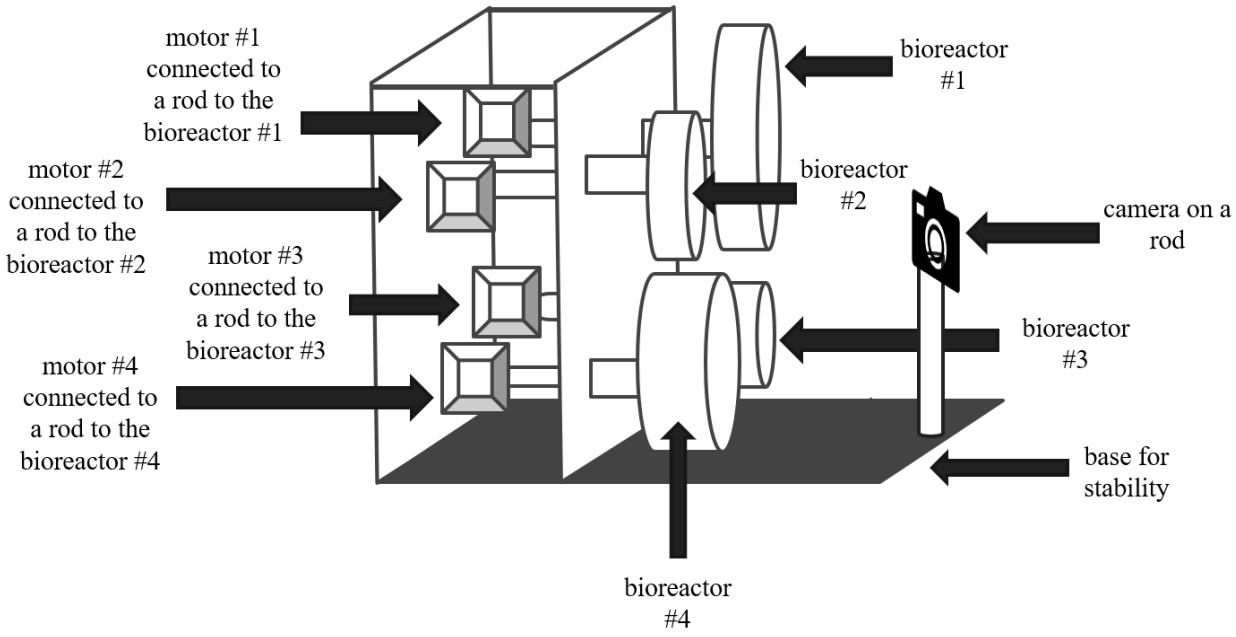

Figure 11. Rough Sketch of the Centrifugation Solution

There are four different bioreactors with different diameters, each attached to a motor. All the bioreactors are held in place by a vertical plane that has holes cut to the size of their diameters. The camera is placed to view the whole circumference of all the bioreactors.

Solution P.C: Inclined Plane (Single Motor)

This proposed solution delineates the utilization of an inclined plane single motor bioreactor, equipped with an integrated webcam monitoring system, as an innovative approach for enhancing the efficiency of cell culture processes. The system is engineered to optimize mixing, oxygen transfer, and gentle agitation—all vital for the proliferation of cells in suspension under partial gravity conditions. These hydrodynamic parameters can be quantitatively characterized using the specific power input (P/V), which correlates motor power with culture volume and serves as an essential metric to ensure proper mixing while preventing excessive shear forces. By maintaining P/V within the ranges established for mammalian and microbial culture systems, the design endeavors to balance nutrient and gas transfer requirements with the safeguarding of sensitive cell cultures [76].

For real-time visualization, the system will incorporate a webcam with adjustable focus and LED illumination to ensure uniform brightfield imaging. To maintain consistent image quality during bioreactor operation, the webcam shall be mounted directly onto the rotating vessel assembly, thereby following the vessel's motion and changes in orientation. This methodology guarantees that the camera sustains a constant field of view relative to the culture. The camera is affixed using a gimbal-like system, which permits the lens to remain aligned with the observation window throughout the entire range of vessel motion.

The control of the bioreactor is overseen by a microcontroller platform, such as Arduino, which regulates motor speed, acquires sensor data, and operates the camera. Data logging facilitates the export of sensor readings and image sequences for subsequent analysis. Safety features comprise over-current protection, temperature cutoffs, and emergency stop mechanisms to ensure the safety of both the vessel and the cultural contents.

The operation of rotation and tilt utilizing a single motor can effectively facilitate controlled vessel rotation; however, it demonstrates limited flexibility in adjusting the vessel's angle. In the simplest configuration, the motor drives the vessel at a fixed RPM while the axis of rotation remains stationary, with the angle relative to gravity mechanically pre-set on the mounting frame. This configuration indicates that the speed and angle cannot be adjusted simultaneously, as the motor can execute only one function at a time. More sophisticated systems, such as differential gears, could be implemented; nonetheless, these systems introduce additional mechanical complexity, thereby reducing overall efficiency [76]. A rough sketch of the solution is seen in Figure 12.

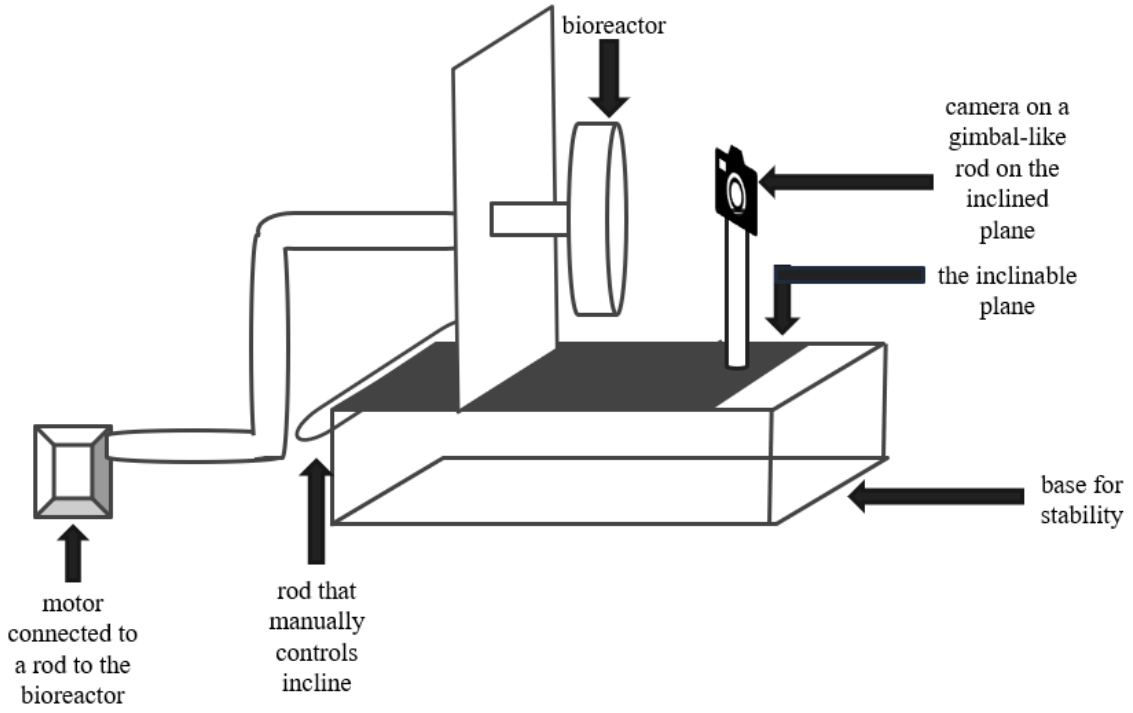

Figure 12. Rough Sketch of Inclined Plane with Single Motor
The figure illustrates the preliminary sketch for the single-motor inclined plane. The bioreactor is connected to the motor via a tube, and the incline plane is adjusted manually.

3.3 Decision Matrix

Selecting the appropriate approach for the bioreactor necessitates evaluating multiple factors, including availability, research utilization, and bubble formation. For the partial gravity scenario, the factors considered are design period, cost, feasibility, and cell viability. Given that each option possesses its own advantages and disadvantages, a weighted comparison is essential to identify the optimal solution. A prioritization (weighted decision) matrix is employed to evaluate the options based on predetermined criteria [77].

Regarding the bioreactor, the primary criterion to consider is availability. Since this prototype comprises two components, with particular emphasis on the partial gravity section, the RWV should not significantly impact the project timeline. Consequently, this criterion is assigned a score of 5 points. A score of 1 indicates that the component is either not accessible or requires design development. In contrast, a score of 2 signifies that it is accessible and does not necessitate any additional design efforts.

The second criterion pertains to research utilization: the number of literature papers that have employed the bioreactor. If research articles have utilized the bioreactor and data extraction occurred without issues, this suggests that the bioreactor is appropriate for use, or that its disadvantages do not outweigh its advantages. Given that the primary objective is to employ the bioreactor for research purposes, this criterion is assigned a weight of three points. A ranking of one indicates minimal usage in the literature, whereas a ranking of two signifies more widespread application.

Finally, the third criterion pertains to the formation of bubbles. Bubble formation represents one of the most limiting factors in data extraction and is therefore assigned a weight of three points. A rank of one indicates that bubble formation is present or disrupts fluid motion, whereas a rank of two signifies that bubble formation does not interfere with the flow of the medium. With these criteria established, the decision matrix is accordingly defined.

Regarding partial gravity, the initial criteria to be considered are the non-negotiable criteria. The primary criterion pertains to the gravitational type (refer to Table 1). Since the main objective is to attain $\frac{1}{6}G$, $\frac{3}{8}G$, $1G$, and μG to verify the locations' gravitational properties that NASA is reluctant to explore, the gravitational type criterion is assigned a weight of 5 points [54][55]. As this criterion requires simulations and theoretical applications, including fluid dynamics and other disciplines, the ranking is based on whether such gravitational values have been tested in previous experiments or through direct mathematical computations. A rank of 1 indicates minimal or no citations, whereas a rank of 3 signifies a higher citation count. The ranking process is conducted for each of the gravitational targets.

The second criterion concerns simulation (see Table 1). In relation to gravity, validation is based on mathematical principles and their effect on an object, considering that gravity is a theoretical framework [57]. The essential criterion states that the method's partial simulation of gravity should not increase shear forces nor disrupt fluid flow, which cannot be validated without simulation. Therefore, the mathematical simulation criterion is assigned 4 points. The ranking of this criterion is determined by its complexity, with 1 indicating the highest complexity and 3 the lowest.

The third criterion is visual validation (refer to Table 1). To confirm that the mathematical simulation accurately represents the system, the visual validation is assigned a weight of 3. The ranking of this criterion depends on the quality of specimen visualization, with 1 indicating difficulty in visualizing the specimen and 3 indicating clear visualization.

The fourth criterion relates to dimensions (refer to Table 1). When the device is situated within the incubator, its size is limited by the dimensions of $21 \times 20 \times 20.8\, in.$ Nonetheless, due to the design's substantial dependence on the type of bioreactor used and considering the restrictions related to dimension ranking, a score of two points is assigned. Consequently, this criterion is assessed based on the likelihood of space utilization, with a ranking of one indicating considerable spatial occupation and a ranking of three indicating minimal space consumption.

The final criterion relates to the project timeline. Considering that the project must be completed within three months, the proposed solution is required to adhere to this schedule. However, due to the dependency of the materials used in the device on procurement schedules and the arrival of supplies, this criterion shall be assigned a weight of 2 points. The ranking for this criterion is based on the ease of project replication, with a score of 1 indicating a prolonged or unprecedented process, and a score of 3 representing a swift completion. Once the criteria are established, the decision matrix is accordingly identified.

After evaluating the criteria for the bioreactor, as presented in Table 3, the standard bioreactor obtained the highest score of 19 points. Consequently, the selected bioreactor is the standard model. Upon assessing the criteria for partial gravity, as shown in Table 4, the inclined plane with dual motors achieved the highest score of 37 points, while the other solutions scored 32 points each. Therefore, the preferred solution is the standard RWV on an inclined plane with dual motors.

Table 3. Design Matrix for RWV Solutions

Criteria	Weight	Standard RWV		Novel RWV	
		Rating	Weighted Score	Rating	Weighted Score
Availability	5	2	10	1	5
Research Usage	3	2	6	1	3
Bubble Formation Disrupts Flow	3	1	3	2	6
Total Score			19		14

The table shows the criteria and weight of each criterion that determines which RWV solution is favorable. The rating and weighted score for each solution are displayed. The standard RWV scored the highest.

Table 4. Design Matrix for Partial Gravity Solutions

Criteria	Weight	Inclined Plane with Dual Motor		Four Centrifugations		Inclined Plane with One Motor	
		Rating	Weighted Score	Rating	Weighted Score	Rating	Weighted Score
Gravitational Type	5	2	10	3	15	2	10
Mathematical Simulation	4	2	8	1	4	2	8
Visual Validation	3	3	9	3	9	2	6
Dimensions	2	2	4	1	2	2	4
Design Time	2	3	6	1	2	2	4
Total Score			37		32		32

The table shows the criteria and weight of each criterion that determines which partial gravity solution is favorable. The rating and weighted score for each solution are displayed. The inclined plane with dual motors scored the highest.

4. Engineering Design

The engineering design of the solution is founded upon detailed methodologies, calculations, and components to facilitate the successful execution of the partial gravity exerted on the cells. This section elucidates the calculations, mechanical plan, electronics, materials, and validation strategies employed to confirm that the selected options align with the system requirements.

4.1 Design Rationale

According to the most essential non-negotiable criteria, the prototype should have the ability to induce at least four different gravitational types: $1G, \frac{3}{8}G, \frac{1}{6}G$, and μG [54][55]. To simulate partial gravity on Earth, various methods, such as parabolic flight, centrifugation, or modified rotation devices, could be used [37].

The parabolic flight methodology allows researchers to conduct experiments under conditions of microgravity and partial gravity, thus simulating lunar or Martian environments in accordance with NASA's mission objective to facilitate human space exploration [78]. The technique utilized to recreate these conditions involves controlled maneuvers that temporarily induce free fall through the following procedures: pull-up, wherein the aircraft ascends at a steep angle (45º) enabling passengers to experience 1.8G; push-over, whereby, upon reaching the apex of the parabolic arc, the pilot reduces engine thrust, causing all objects inside the aircraft to descend together; reduced gravity, which occurs during the descent when no force acts upon the occupants, creating weightless conditions similar to those in space; and pull-out, where increased engine thrust and leveling out return the aircraft to Earth's gravity [78]. However, this approach has several limitations, including the short duration of reduced gravity, approximately 20 seconds per parabola, with typical flights comprising between 15 and 30 parabolas [78].

Centrifugation is employed to modify the magnitude of Earth's gravitational force in accordance with Einstein's Equivalence Principle, demonstrating that there exists no physical distinction between acceleration due to mass and linear acceleration [79, 80]. Operating a centrifuge at a constant velocity enables the sample to continually alter its direction and remain centered within the rotation [79]. Recognizing that the inertia of the sample and the rotation of the centrifuge collectively generate gravitational effects, the magnitude of this simulated gravity is dependent on the radius of the centrifuge and its angular velocity [79]. Centrifuges are utilized to mimic microgravity conditions through the Reduced Gravity Paradigm (RGP), which emphasizes the responses elicited by the difference between two levels of acceleration. RGP is most effective when applied to a stable and steady system operating at a high gravitational level before reducing the acceleration, with optimal results observed in systems that respond rapidly, as intermediate and slow responding systems require more extended periods than the available time interval to achieve the desired gravity level.

Given the significance of stability in centrifugation, modified rotational devices, including bioreactors, are assessed for their efficacy in partial gravity simulation. Bioreactors are biomechanically active systems engineered to replicate biological conditions by utilizing mechanical means to influence cellular processes through the meticulous regulation of biochemical and physical signals [81]. RWV, which employs vessel

rotation to generate low-shear mixing and simulated microgravity within the chamber, is available in two variants: the slow-turning lateral vessel (STLV) and the high aspect ratio vessel (HARV), as illustrated in Figure 13 [82]. The differences between these two types include the fact that STLVs incorporate a central cylinder oxygenator and can accommodate larger volumes. In contrast, HARVs are equipped with a gas-permeable member on one of their walls to enhance oxygenation [83][84][85].

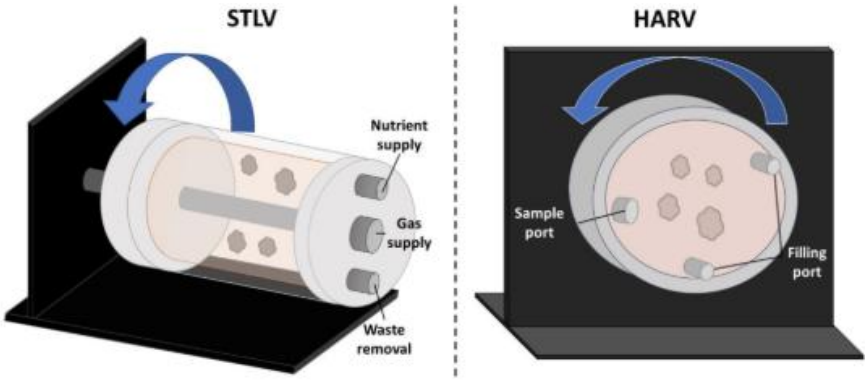

Figure 13. STLV vs HARV
The figure on the left depicts the STLV bioreactor, with its ports clearly labeled. To the right, the HARV is displayed, also with labeled ports. A cylindrical shape characterizes the STLV, whereas the HARV has a disc-shaped configuration [82].

Despite the limitations associated with the RWV, which include the requirement for high user competency, bubble formation, and the difficulty in determining the appropriate rotational speed to balance solid-body rotation with continuous freefall, the device enhances cellular performance through its capacity to improve mixing in low-shear environments substantially, facilitate high-density cell cultures and self-aggregation, promote cellular differentiation, and, notably, simulate microgravity. The effects of this simulation are well documented, encompassing alterations in calcium handling within cardiac cells and interference with cellular differentiation pathways [86][87][88].

The proposed solution emphasizes the integration of various benefits associated with different types of partial gravity simulation, while maintaining minimal adverse effects. To optimize cell growth, it is essential to cultivate cells in a manner that simulates free-fall. Consequently, maintaining a constant and steady rotation of the cells is necessary to ensure continuous exposure to free-fall conditions. This objective can be achieved by modifying the rotation of the RWV through the integration of centrifugation methods. As depicted in Figure 14, the device's orbit will be controlled to ensure a low-shear environment with a balanced solid-body rotation and continuous free-fall conditions [89].

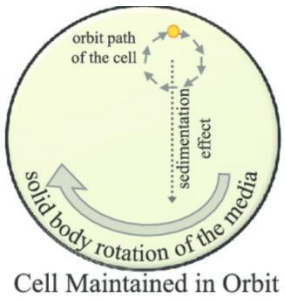

Figure 14. Orbit Trajectory of the Cell Within a Rotating Bioreactor

The orbital trajectory of the cell within a rotating bioreactor. The sustained rotation and sedimentation effects prevent the cells from settling at the base of the vessel. Additionally, the clockwise rotation of the medium facilitates the continuous suspension of cells in the orbit [89].

However, the centrifugation process would not accurately simulate the partial gravity of $\frac{1}{6}G$ and $\frac{3}{8}G$. With the inclination in the parabolic flight enabling a 1.8G simulation, the inclined plane within the solution would serve as the primary mechanism to achieve partial gravity conditions. In fact, NASA is presently constructing a Mars Artificial Gravity Habitat with Centrifugation (MAGICIAN) module to emulate Earth's gravity on Mars, as illustrated in Figure 15 [90].

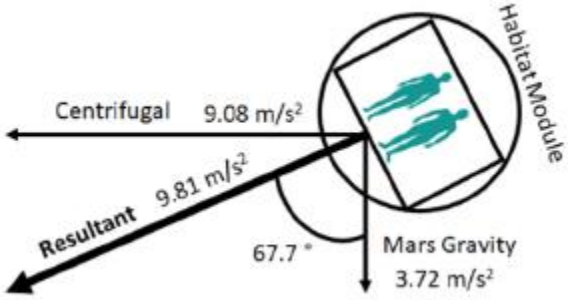

Figure 15. MAGAICIAN Schematic

A two-dimensional cross-section of the MAGIGAN modules displayed at an angle of 67.7° to achieve a resultant force equivalent to Earth's gravity [90].

Using a bioreactor would provide a controlled environment for cell growth, reducing the chances of inaccurate data caused by cell culture. Given that the bioreactor's rotation is maintained at a constant rate and the inclined plane's movement is solely a result of gravitational simulation, two motors will be employed. These motors will be identical to minimize potential complications in coding or wiring.

4.2 Calculations

To construct the prototype, specific calculations must be performed. These calculations will be utilized for simulation purposes to validate the prototype. To generalize the calculation, the specimen will be referred to as a particle; however, it pertains to cells and the samples used during validation. Due to the numerous considerations involved in the calculation, the process will be divided into five sections: the inclined plane, sedimentation velocity, angular velocity, revolutions per minute, and cellular portion.

Incline Plane

The inclined plane facilitates the reduction of the gravitational force exerted on a particle by decomposing it into components. Referring to Figure 16, the gravitational force is entirely on one axis when $\theta° = 0° \; or \; 90°$ or decomposed into components. Utilizing trigonometry, Eq. 2 and Eq. 3 illustrate the values for the parallel and perpendicular components of gravity relative to the base [91].

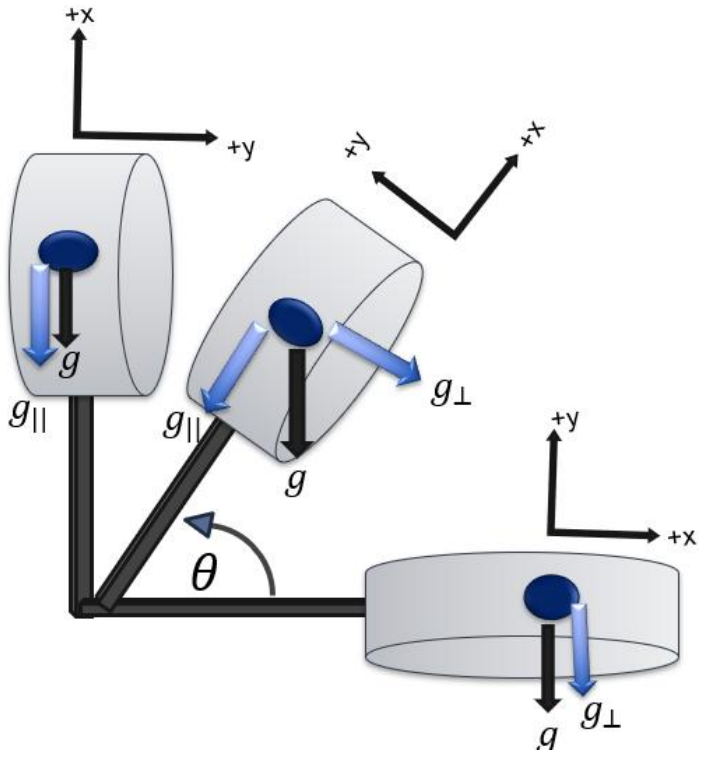

Figure 16. Free Body Diagram of a Bioreactor on an Inclined Plane
When the plane is parallel to the base, the gravitational force acts in the y-direction. When the plane is inclined at an angle θ from the base, the gravitational force is resolved into components. When the plane is perpendicular to the base, the gravitational force acts in the y-direction. The blue arrows represent the components of the gravity present in each scenario.

$$g_{\parallel} = g \sin \theta° \quad (2)$$

Equation 2. Parallel Gravitational Component

Where:
$g_{\parallel}$ = gravitational component parallel to the base
g = c
$\theta°$ = angle between the inclined plane and the base

$$g_{\perp} = g \cos \theta° \quad (3)$$

Equation 3. Perpendicular Gravitational Component (Tangential Gravity)

Where:
$g_{\perp}$ = gravitational component perpendicular to the base (intended gravity)
g = $g_{\perp} = g \cos \theta°$
$\theta°$ = angle between the inclined plane and the base

Given that the bioreactor remains stable along the x-axis, i.e., it does not slide on the inclined plane, $g_{\parallel}$ is utilized for the centrifugation process of the bioreactor. Regarding $g_{\perp}$, it represents the normal force, which serves as the weight; reducing this force would simulate a decreased weight on the cells. Consequently, $g_{\perp}$ denotes the intended gravitational force. Therefore, by solving Eq. 3 in terms of θ, Eq. 4 delineates the angle of the inclined plane pertinent to the effective gravitational force equation.

$$\theta = \cos^{-1}(\frac{g_{\perp}}{g}) \quad (4)$$

Equation 4. Inclined Plane Angle

Where:
$g_{\perp}$ = gravitational component perpendicular to the base (intended gravity)
g = Earth's gravity ($9.81 \frac{m}{s^2}$)
$\theta°$ = angle between the inclined plane and the base

Although the inclination angle equation establishes the environment in which the particle experiences modified gravitational forces, the particles should be in a state of "free fall" at any inclination position. Therefore, the calculation of the centripetal acceleration is necessary.

Centripetal Acceleration

Given that uniform and steady circular motion is requisite for laminar flow, centripetal acceleration will be employed. The centripetal acceleration (a_c) is directed towards the center, with the sole opposing acceleration being $g_{\parallel}$. Therefore, the accelerations should be counteracting to ensure that no net force is exerted on the particle, as demonstrated in Eq. 5, with Eq. 2 and the substitution of the relevant quantities for a_c.

$$a_c = g_{\parallel} \Longrightarrow$$
$$\omega^2 R = g \sin\theta° \quad (5)$$

Equation 5. Net Horizontal Acceleration

Where:
ω = angular velocity
g = Earth's gravity ($9.81 \frac{m}{s^2}$)
$\theta°$ = angle between the inclined plane and the base
R = radius of rotation of the particle to the center

Following the establishment of the connection for a_c, ω can be subsequently calculated.

Angular Velocity

Following the manipulation of Eq. 5, Eq. 6 was employed to isolate the angular velocity.

$$\omega = \sqrt{\frac{g \sin\theta°}{R}} \quad (6)$$

Equation 6. Modified Angular Velocity

Where:
ω = angular velocity
g = Earth's gravity ($9.81 \frac{m}{s^2}$)
$\theta°$ = angle between the inclined plane and the base
R = radius of rotation of the particle to the center

RPM

Utilizing Eq. 7, the relationship between RPM and angular velocity is demonstrated [92].

$$RPM = \frac{60\omega}{2\pi} \quad (7)$$

Equation 7. RPM

Where:
RPM = revolutions per minute
ω = angular velocity

Substituting Eq. 6 into Eq. 7, Eq. 8 shows the RPM for the bioreactor.

$$RPM = \frac{60}{2\pi}\sqrt{\frac{g \sin\theta^\circ}{R}} \quad (8)$$

Equation 8. Bioreactor RPM

Where:
RPM = revolutions per minute
g = Earth's gravity ($9.81\frac{m}{s^2}$)
θ° = angle between the inclined plane and the base
R = radius of rotation of the particle to the center

The rotation of the bioreactor could be subsequently calculated. However, one of the limiting factors in its rotation is the linear velocity induced by the fluid moving tangentially. Therefore, it is necessary to determine the linear velocity of the system.

Linear Velocity

The fluid within the bioreactor exhibits tangential movement concurrent with rotation. Eq. 9 illustrates the relationship between angular velocity and linear velocity [92].

$$v = \omega R \quad (9)$$

Equation 9. Linear Velocity in Terms of Angular Velocity

Where:
ω = angular velocity
v = linear velocity
R = radius of rotation of the particle to the center

By substituting Eq. 6 into Eq. 9, Eq. 10 illustrates the linear velocity of the bioreactor.

$$v_{\perp} = \sqrt{Rg \sin \theta^{\circ}} \tag{10}$$

Equation 10. Tangential Velocity

Where:

$v_{\perp}$ = tangential velocity

g = Earth's gravity ($9.81 \frac{m}{s^2}$)

θ° = angle between the inclined plane and the base

R = radius of rotation of the particle to the center

Given that the fluid possesses its tangential velocity, the particles suspended within the fluid exhibit their sedimentation velocity. To facilitate "free-fall" conditions for the particles, the sedimentation velocity must be computed.

Sedimentation Velocity

Sedimentation velocity refers to the terminal velocity of a particle within a quiescent fluid [92]. At this velocity, the particle experiences no acceleration, as its terminal velocity remains steady. Utilizing Stokes's law, the upward drag force resisting the particle's descent must be equal to the downward gravitational force [93]. However, Stokes's law is predicated upon three fundamental assumptions:

1) The particle is small and spherical.
2) The particle does not rotate within the fluid.
3) Reynold's number is considerably less than 1.

Although cells are not perfectly spherical, Stokes' law provides an approximate estimation of the terminal velocity. Referring to Figure 17, the particle is suspended within the fluid; therefore, the net force exerted on the particle can be calculated as shown in Eq. 11.

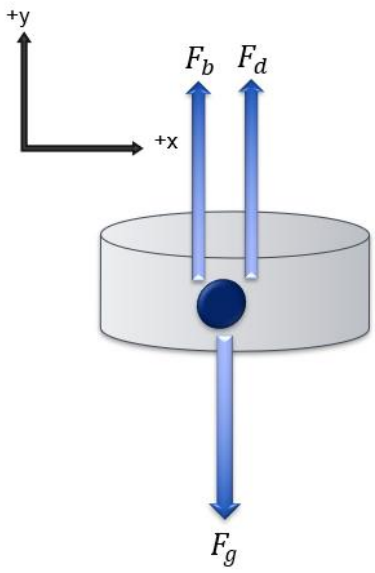

Figure 17. Free Body Diagram of the Particle in Fluid

The figure illustrates the forces acting upon the particle during its suspension within the fluid.

$$F_g = F_b + F_d \tag{11}$$

Equation 11. Net Driving Force on the Particle

Where:

F_g = gravitational force exerted on the particle

F_b = buoyancy force exerted on the particle

F_d = drag force exerted on the particle

Eq. 12 and Eq. 13 show the equivalence of the gravitational force (F_g) in a fluid and the buoyancy force (F_b), respectively [93].

$$F_g = V * \rho_p * g_\perp \tag{12}$$

Equation 12: Equivalence of Gravitational Force

Where:

F_g = gravitational force exerted on the particle

V = volume of the particle

ρ_p = density of the particle

$g_\perp$ = gravitational component perpendicular to the base (intended gravity)

$$F_b = V * \rho_f * g_\perp \quad (13)$$

Equation 13: Equivalence of Buoyancy Force

Where:
F_g = gravitational force exerted on the particle
V = volume of the particle
ρ_f = density of the fluid
$g_\perp$ = gravitational component perpendicular to the base (intended gravity)

Assuming that the particle's shape is spherical, the volume of the sphere is determined as shown in Eq. 14.

$$V_s = \frac{4}{3}\pi r^3 \quad (14)$$

Equation 14: Volume of Sphere

Where:
V_s = volume of the sphere
r = radius of the sphere

The drag force under consideration is that exerted on a spherical particle, as demonstrated in Eq. 15 [93].

$$F_d = 6\pi r \eta_f v_t \quad (15)$$

Equation 15: Drag Force

Where:
F_d = drag force exerted on the particle
r = radius of the particle
η_f = fluid viscosity
v_t = sedimentation velocity

Utilizing Eqs. 12-15, Eq. 16 is derived as the fully substituted form of Eq. 11.

$$F_g = F_b + F_d \implies$$
$$V_s * \rho_p * g_\perp = V_s * \rho_f * g_\perp + 6\pi r \eta_f v_t \implies$$
$$\frac{4}{3}\pi r^3 * \rho_p * g \cos\theta° = \frac{4}{3}\pi r^3 * \rho_f * g \cos\theta° + 6\pi r \eta_f v_t \qquad (16)$$

Equation 16: Fully Derived Net Driving Force on the Particle

Where:
r = radius of the particle
ρ_p = density of the particle
g = Earth's gravity ($9.81 \frac{m}{s^2}$)
$\theta°$ = angle between the inclined plane and the base
ρ_f = density of the fluid
η_f = fluid viscosity
v_t = sedimentation velocity

The sedimentation velocity equation, as seen in Eq. 17, is derived from Eq. 16 [92].

$$v_t = \frac{2}{9*\eta_f}(\rho_p - \rho_f) * r^2 * g \cos\theta° \qquad (17)$$

Equation 17: Sedimentation Velocity

Where:
v_t = sedimentation velocity
r = radius of the particle
ρ_p = density of the particle
g = Earth's gravity ($9.81 \frac{m}{s^2}$)
$\theta°$ = angle between the inclined plane and the base
ρ_f = density of the fluid
η_f = fluid viscosity

However, the values derived from the settling velocity are based on various assumptions. To ensure that the particle remains in laminar motion, thereby validating the prior calculations of sedimentation velocity, the particle Reynolds number (Re_p) should be less than 1 [94]. By employing Eq. 18, the calculations can be verified by calculating the Re_p, as all sedimentation velocity computations were predicated on laminar flow.

$$Re_p = \frac{\rho_f * v_t * 2 * r}{\eta_f} < 1 \quad (18)$$

Equation 18. Particle Reynolds Number

Where:
Re_p = particle Reynolds number
ρ_f = density of the fluid
v_t = sedimentation velocity
r = radius of the particle
η_f = fluid viscosity

Cellular Portion

To enhance the mathematical model and provide more accurate RPM values, certain cellular aspects should be considered. These include cell expansion over time, as described in Eq. 19, and cell growth over time, as indicated in Eq. 20, which would serve to improve the mathematical precision [95].

$$V(t) = V_o e^{ln2(\frac{t_d}{T})} \quad (19)$$

Equation 19. Cell Expansion Over Time

Where:
$V(t)$ = cell expansion over time
V_o = initial volume of cells
T = species/condition-specific interval between volume doublings
t_d = time since the last division

$$N(t) = N_o e^{rt} \quad (20)$$

Equation 20. Cell Growth Over Time

Where:
$N(t)$ = cell growth over time
N_o = initial number of cells in the population
t = time
r = population growth rate

4.3 Numerical Sampling

Numerical sampling shall be employed to validate the equations extracted in the Calculations section. However, before calculating theoretically, some basis for the assumption should be discussed to validate the results. RPM values from 0 rpm to 1300 rpm are expected [97]. An rpm of 1300 is anticipated to be extreme, with a maximum exposure duration of 10 minutes to cells before their death [97]. As for Re_p being less than 1, there is a high possibility of cells flowing in laminar flow, such as endothelial cells in blood flow [98][99].

Given that osteoblasts are the most frequently used cells for the validation of partial gravity in culture systems, the particle considered within the system would be an osteoblast cell [100][101]. As this represents first-order numerical sampling, cell-to-cell interactions have not yet been incorporated into the model. Consequently, it will be assumed that the cells do not interact with one another.

The osteoblasts possess a diameter ranging from 20 to 50 micrometers [102]. Considering that cellular water content varies between 60% and 80%, the cell density marginally exceeds that of water, which is estimated at approximately 1.050 $\frac{g}{cm^3}$ [103]. Since the cells are predominantly cultured in Dulbecco's Modified Eagle Medium (DMEM) supplemented with 5% fetal bovine serum (FBS), the density is 1.005 $\frac{g}{cm^3}$, and the viscosity is characterized as $0.862 mPa.s$ [104][105].

Since there are two possible bioreactors used in this project, the smallest and largest diameters would be considered. The HARV has a diameter of 18.30mm (for 1mL) and 99.06mm (for 50mL), while STLV has a diameter of 57.15m (for 55mL) and 95.25mm (for 1000mL) [106][107].

Consequently, numerical values could be determined. Given the presence of multiple variables, a code (refer to Supplementary Code S 1) was employed to obtain the results, as shown in Table 5.

Table 5. Numerical Values of Theoretical Cell Culture

Gravity ($\frac{m}{s^2}$)	Inclined Angle (°)	Bioreactor	Bioreactor Radius (m)	RPM ($\frac{rev}{min}$)	$v_\perp$ ($\frac{m}{s}$)	v_t ($\frac{m}{s}$) (small cells)	v_t ($\frac{m}{s}$) (large cells)	Re_p (small cells)	Re_p (large cells)
9.807	0.000	HARV	0.009150	312.6	0.000	$4.6*10^{-5}$	$2.8*10^{-4}$	0.013	0.033
1.634	80.41	HARV	0.04953	54.86	0.6920	$7.6*10^{-6}$	$4.7*10^{-5}$	0.0022	0.0055
3.677	67.98	SLTV	0.02857	108.3	0.5097	$1.7*10^{-5}$	$1.1*10^{-4}$	0.0050	0.012
9.807	89.99	SLTV	0.04763	0.1370	0.6834	$4.6*10^{-11}$	$2.8*10^{-10}$	$1.3*10^{-8}$	$3.3*10^{-8}$

The table presents some of the final numerical values derived from the equations detailed in the Calculation section. Not all conditions have been evaluated. The table includes four different values of gravity and their respective incline angles, along with the RPM corresponding to a specific bioreactor radius. From this data, the tangential velocity of the system, the sedimentation velocity of the cells, and the Reynolds number for the cells were subsequently calculated.

All the particle Reynolds numbers were less than 1, indicating laminar flow and confirming the validity of the calculation process. The inclined angles correspond to accurate data, with no inclination relative to Earth's gravity and a perpendicular orientation to the surface in microgravity. However, some values exceed the anticipated RPM values; therefore, specific correlations should be considered.

Correlation and Analysis

After calculating both the sedimentation velocity and the tangential velocity, the ratio of these velocities offers valuable insights into the interactions among the particles within the fluid. If the sedimentation velocity surpasses the tangential velocity, it indicates that the particles would settle, which is undesirable. Conversely, if the terminal velocity is lower than the tangential velocity, it suggests that the particles remain in suspension continuously. The objective is to ensure that the tangential velocity exceeds the terminal velocity. Eq. 21 illustrates the velocity ratio and its associated conditions. If this condition is not satisfied, resulting in an infinite or undefined ratio, adjustments to the system should be implemented.

$$v_t \ll v_\perp$$
$$\frac{v_t}{v_\perp} \ll 1 \qquad (21)$$

Equation 21. Velocity Ratio

Where:
$v_\perp$ = tangential velocity
v_t = sedimentation velocity

Currently, it is not feasible to modify the RPM or the angle without affecting the gravitational effects. Nevertheless, the equations offer several correlations.

Figure 18A shows the correlation of the RPM with the inclined angle. The correlation is

$$RPM \propto \sin\theta$$

, considering the radius is kept constant. Therefore, as the angle increases, the RPM increases.

Figure 18B shows the correlation of the RPM with the radius. The correlation is

$$RPM \propto \frac{1}{\sqrt{R}}$$

, considering the angle is kept constant. Therefore, as the radius increases, the RPM decreases.

A. **B.**

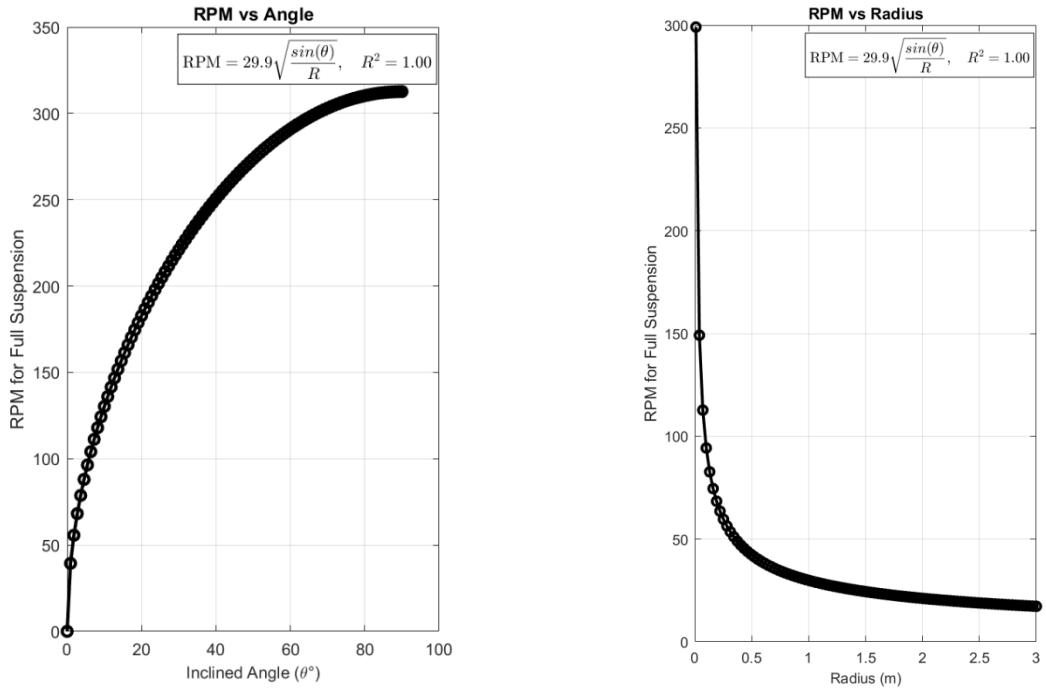

Figure 18. RPM vs Angle and Radius
(A) The figure demonstrates that increasing the angle increases RPM. (B) The figure illustrates that increasing the bioreactor radius decreases RPM.

4.4 Simulation

Given the presence of first-order mathematical equations, a simulation can be conducted.

Mathematical Simulation

To mathematically simulate the equations presented in the Calculation section, two approaches are employed: coding. Utilizing Supplementary Code S 1 as the foundation of the simulation, a starter code is given.

To enhance the user interface, the user will be prompted to specify options for the calculations. The criteria for these prompts will include gravity type, bioreactor type, particle type, and medium used.

Specific criteria are associated with sub-criteria. The categories of gravity type and bioreactor type have no sub-criteria. Conversely, the particle type encompasses two sub-criteria: particle radius and particle density. The medium type has two sub-criteria: viscosity and density of the medium. Options for each criterion are pre-coded based on their prevalence, as determined from literature sources. For instance, if a user selects DMEM + 5% PBS as the medium, the viscosity and density values would be pre-coded accordingly, for example, as $1.005\ \frac{g}{cm^3}$ and $0.862 mPa.s$, respectively [104][105]. In cases where the pre-

coded options do not suit the user's requirements, an “Other” option is available. When a criterion includes sub-criteria, the user will be prompted to input the relevant details.

The Reynolds number will be calculated using Eq. 18. If the value exceeds 1, a message will indicate that the flow is non-laminar. Since this is starter code, no further calculations will be performed due to the lack of understanding of the motion if it is not laminar. If the value is less than or equal to 1, the velocity ratio will be calculated using Eq. 21. If the ratio exceeds 1, a message will state that the particle would settle. If the ratio is less than 1, a message will say that the particle will stay suspended continuously. Further research is needed to understand the implications of a ratio if it is not less than 1. For now, calculations will continue only if the ratio is less than 1.

The inclinations are calculated using Eq. 4. Gravitational components are derived from Eqs. 2 and 3. The angular velocity is obtained from Eq. 6. RPM is calculated with Eq. 8. The tangential velocity is determined using Eq. 10. Sedimentation velocity is obtained from Eq. 17. All calculations are performed automatically and displayed to the user.

4.5 Components

After understanding roughly how the system would work, the mathematical aspect would allow the choice of the right components.

One of the most critical aspects of the prototype is the bioreactor. Choosing between the HARV and STLV bioreactors, there are two crucial factors: radius and view clearance. Using Eq. 8, the RPM for the smallest radius (belonging to HARV) and the largest radius (belonging to STLV) was calculated. Using Eq. 22, the percentage difference was 79.7%.

$$\frac{|A-B|}{\frac{(A+B)}{2}} \tag{22}$$

Equation 22. Percent Difference

Where:
$A =$ first value
$B =$ second value

Looking at Figure 19, there is a decrease in RPM with the increase of radius for the same gravitational condition, supported by the relationship concluded from Figure 18.B.

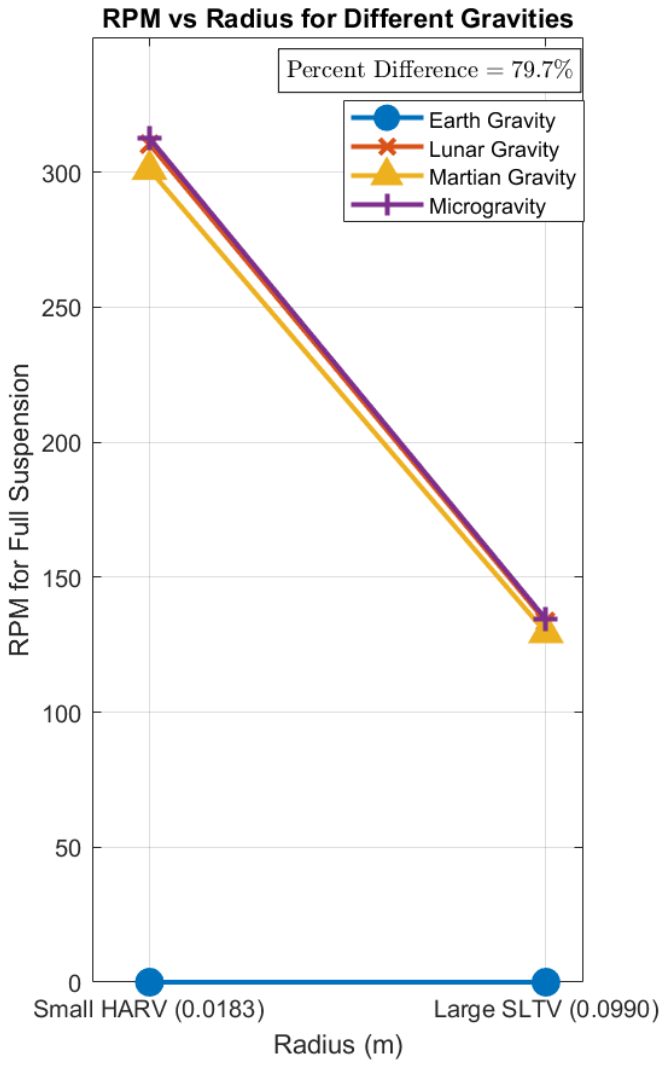

Figure 19. RPM vs Smallest and Largest Radii Measurements for the STLV and HARV Bioreactors

Given that a maximum of 1300 rpm is considered extreme when sustained for more than 10 minutes, as exceeding this limit could result in the denaturation of cells, a smaller radius is preferable for maintaining healthy cell cultures [97]. Consequently, the bioreactor with the smallest radius is deemed the optimal choice. However, since Dr. Lelkes' laboratory provides the bioreactors, the final selection has not yet been made. Regarding view clearance, a significant aspect of the prototype involves visually assessing the particle during rotation and inclination. Therefore, the bioreactor chosen should have a small radius and a large view area. The camera has yet to be selected, depending on the bioreactor that will be utilized.

As for the motor, to find the intended torque, Eq. 23 is used by plugging in Eq.7 to solve for ω and Eq. 5 to solve for a_c.

$$\tau = m * R_b * a_c \implies \tau = m * R_b * \omega^2 * R_b \implies \tau = m * {R_b}^2 * (\frac{2\pi}{60} * RPM)^2 \quad (23)$$

Equation 23. Torque

Where:
τ = torque
m = mass
R_b = radius of rotation of the particle to the center
RPM = revolution per minute

Having a safety factor of 2, the torque equation will be multiplied by 2. To get the power, Eq. 24

$$P = \omega * \tau \implies P = \frac{2\pi}{60} * RPM * \tau \quad (24)$$

Equation 24. Power

Where:
τ = torque
P = power
RPM = revolution per minute

The calculations shall be conducted based on the most adverse scenario. The maximum values for mass, radius, and RPM are 3.00 kg, 0.0495 m, and 313 rpm, respectively. The mass was obtained from the calculations of the previous senior design team. The torque and power computed using Eqs. 23 and 24 are 7.89 Nm and 259 W, respectively. The safety torque is 11.8 Nm.

A suitable motor option is the NEMA 34 stepper motor, which possesses a torque of 12 Nm and a 1.8° step [108]. When selecting this motor, the microstep driver employed must be compatible. The microstep driver enhances the stepper motor's precision and ensures smoother operation. The DM86OH is compatible with a DSP driver characterized by low noise levels [109]. The compatible microcontroller selected for this application is the Arduino Nano, featuring the ATMega4809 processor, which provides greater programmability compared to the Arduino Uno, along with increased program memory and RAM [110].

5. Test Method

To guarantee the validity of the results and decisions, specific tests must be conducted.

5.1 Bioreactor Radius

To choose the bioreactor for the prototype, the radius should be considered. Figure 19 shows that the radius significantly affects RPM. For that reason, the smallest radius is the choice. However, there are samples of bioreactors that will be provided. For that, the test method helps determine which bioreactor to use.

All bioreactors will have a tape affixed to their circumference. Using a marker and a ruler, a tick will be inscribed at the most extreme opposite ends of each bioreactor's circumference with a black marker. Each bioreactor will have at least three pairs of ticks: along the center diameter, another at the center diameter, and a 45-degree diameter from any of the previous ones. Three measurements of each tick pair will be obtained utilizing a caliper. These measurements will be documented in an Excel file. Additionally, the same tick pairs will be analyzed using ImageJ software. To ensure there is no significant discrepancy between the measurements, a student's t-test will be performed on each dataset. In the event of a significant difference, the protocol will be repeated. Once insignificant differences are confirmed, the data will be transferred to JMP software for analysis, and a student's t-test will be conducted to determine if there are significant differences in the radii of the bioreactors.

A decision shall be made after the measurement of the radii of the available bioreactors.

5.2 Visual Assessment Camera Placement

The visual validation mainly relies on clearly positioning the camera so that the interior of the bioreactor is visible. For this purpose, the protocol is established.

Utilizing at least two distinct phone cameras, three photographs will be captured from each viewpoint, with the camera parallel to the circular side of the bioreactor, as assessed by the observer. Using a ruler, the distance between the camera and the bioreactor will be documented in an Excel file. For every bioreactor, at each viewpoint, a minimum of three photographs will be taken at three different magnifications. This methodology aims to provide a broader range of magnification options, considering that the camera has not yet been acquired. Each image will be imported into MATLAB, and photo analysis will be employed to identify the visible area. The area values will subsequently be analyzed in JMP using the Fit Model procedure to assess statistical significance. Ultimately, the largest statistically significant area will be used to determine the optimal camera distance and magnification.

A decision shall be made after the measurement of the areas of the camera choice.

5.3 Validation of Fluid Dynamics Using Alginate Beads

To validate the partial-gravity bioreactor and fluid dynamics, alginate beads can be added to visualize the motion of particles. Developed from a calcium chloride solution, they have similar densities to that of a cell. Due to the increased size of alginate beads, the bioreactor would have to run at 15 rpm.

The alginate beads do not confirm the existence of a partial-gravity environment; however, they accurately represent the forces and fluid dynamics occurring within the novel bioreactor to verify that an appropriate environment is being created within the device. This validation will directly influence whether it is possible to culture cells within the bioreactor.

6. Progress

Throughout all weeks, any progress that occurs and is to be included in the final paper shall be incorporated into the document on the same day, and the paper shall be submitted to the advisor by the end of the week for review to ensure that no modifications are required. The same procedure applies to the presentation.

6.1 Week 4

Week #4 marks the midterm week for certain members of our group. To prevent falling behind due to impractical deadlines, no urgent tasks are scheduled for this week. The objectives for this week are to:

1. Do the first two test methods
2. Fix the dimensions of the incubator
3. Include validation testing methods in the paper (link to criteria).
4. Add more mathematical equations to improve the accuracy of cell modeling.
5. Find modifications to Stokes' Law for a more accurate settling velocity.
6. Understand how to incorporate time into the equations now found.
7. Find CAD parts for the CAD drawing.
8. Create a CAD drawing of the prototype.
9. Search for parts and create a cost table with a total under $1000.

Since there are four people in the team, the tasks will be divided as follows:

Task	Person in Charge	Due
#1	Members in Temple	Friday Sept. 26
#2	Members in Temple	Friday Sept. 26
#3	All Members	Friday Sept. 26
#4	All Members (together)	Monday Sept. 29
#5	All Members (group chat)	Wed. Oct 1
#6	Jake	Friday Oct. 3
#7	Dmitry and Zenub	Friday Oct. 3
#8	Zenub	Friday Oct. 3
#9	Dmitry and Zenub	Friday Oct. 3

6.2 Week 5

Week #5 is designated as the period by which all tasks assigned in Week #4 are anticipated to be concluded. The objectives for this week are to:

1. Search for parts and create a cost table with a total under $1000.
2. Find CAD parts for the CAD drawing.
3. Create a CAD drawing of the prototype.
4. Add more mathematical equations to improve the accuracy of cell modeling.
5. Find modifications to Stokes' Law for more accurate settling velocity.
6. Understand how to incorporate time into the equations now found.

Since there are four people in the team, the tasks will be divided as follows:

Task	Person in Charge	Due
#1	All Members (together)	Monday Sept. 29
#2	All Members (group chat)	Wed. Oct 1
#3	Jake	Friday Oct. 3
#4	Dmitry and Zenub	Friday Oct. 3
#5	Zenub	Friday Oct. 3
#6	Dmitry and Zenub	Friday Oct. 3

6.3 Week 6

With the CAD drawing completed, we aim to have a prototype ready by Week #6. The objectives for this week are to:

1. Order parts after advisor approval.
2. 3D-print the prototype's base.
3. Check if there are any adjustments needed in the system or if we're missing any parts.
4. Continue improving the mathematical model.

Since there are four people in the team, the tasks will be divided as follows:

Task	Person in Charge	Due
#1	Irene	Monday Oct. 6
#2	Jake	Tuesday Oct. 7
#3	All Members	Wednesday Oct. 8
#4	Dmitry and Zenub	Friday Oct. 10

7. References

1) "April 1961 - First Human Entered Space - NASA," NASA. Available: https://www.nasa.gov/image-article/april-1961-first-human-entered-space/

2) "Croatian Barrel Theory," Google Books. Available: https://books.google.com/books?hl=en&lr=&id=6fpgEQAAQBAJ&oi=fnd&pg=PR3&dq=why+are+the+rings+around+the+planets+for&ots=6NYg8vGXx7&sig=fDnYWiJSO_0-C7OTs6DVDOnjzG8#v=onepage&q=why%20are%20the%20rings%20around%20the%20planets%20for&f=false

3) "Croatian Barrel Theory | Miro (Mike) Laus," Mike Laus. Available: https://www.miromikelaus.com/#:~:text=Grounded%20in%20Laus%E2%80%99s%20cultural%20heritage%2C%20the%20Croatian%20Barrel,system%2C%20with%20celestial%20bodies%20emerging%20at%20varying%20times.

4) A. May, "10 Wild Theories About the Universe," Live Science, Jul. 16, 2021. Available: https://www.livescience.com/strange-theories-about-the-universe.html

5) R. H. Sanders and S. S. McGaugh, "Modified Newtonian Dynamics as an Alternative to Dark Matter," Annual Review of Astronomy and Astrophysics, vol. 40, no. 1, pp. 263–317, Sep. 2002, doi: 10.1146/annurev.astro.40.060401.093923. Available: https://doi.org/10.1146/annurev.astro.40.060401.093923

6) B. Famaey and A. Durakovic, "Modified Newtonian Dynamics (MOND)," arXiv.org, Jan. 28, 2025. Available: https://arxiv.org/abs/2501.17006

7) NASA, "Studying Combustion and Fire Safety - NASA," NASA, Mar. 07, 2024. Available: https://www.nasa.gov/missions/station/iss-research/studying-combustion-and-fire-safety/

8) Gullari, Jeevan Kumar. (2025). The Impact of Moon Phases on Earth, Plants, and Humans: A Comprehensive Study from Project Alpha. 10.13140/RG.2.2.12235.71203. Available: https://papers.ssrn.com/sol3/papers.cfm?abstract_id=5090101

9) J. Green, D. Draper, S. Boardsen, and C. Dong, "When the Moon Had a Magnetosphere," Science Advances, vol. 6, no. 42, Oct. 2020, doi: 10.1126/sciadv.abc0865. Available: https://pmc.ncbi.nlm.nih.gov/articles/PMC10763664/

10) A. Cermak, "Mars Exploration - NASA Science," NASA Science, Aug. 01, 2025. Available: https://science.nasa.gov/planetary-science/programs/mars-exploration/

11) "Why Go to Mars?" Available: https://www.esa.int/Science_Exploration/Human_and_Robotic_Exploration/Exploration/Why_go_to_Mars#:~:text=The%20scientific%20reasons%20for%20going%20to%20Ma

rs%20can,beyond%20Earth%20is%20a%20fundamental%20question%20of%20humankind.

12) J. T. Fisher, U. Ciuha, P. Denise, A. C. McDonnell, H. Normand, and I. B. Mekjavic, "The Combined Effects of Artificial Gravity, Temperature, and Hypoxia on Haemodynamic Responses and Limb Blood Flow," European Journal of Applied Physiology, Apr. 2025, doi: 10.1007/s00421-025-05773-7. Available: https://doi.org/10.1007/s00421-025-05773-7

13) S. A. Narayanan, "Gravity's Effect on Biology," Frontiers in Physiology, vol. 14, Jul. 2023, doi: 10.3389/fphys.2023.1199175. Available: https://pmc.ncbi.nlm.nih.gov/articles/PMC10351380/

14) E. R. Morey-Holton, "The Impact of Gravity on Life," in Elsevier eBooks, 2003, pp. 143–159. doi: 10.1016/b978-012598655-7/50036-7. Available: https://www.sciencedirect.com/science/article/pii/B9780125986557500367?via%3Dihub

15) M. L. Lewis et al., "cDNA Microarray Reveals Altered Cytoskeletal Gene Expression in Space-Flown Leukemic T Lymphocytes (Jurkat)," The FASEB Journal, vol. 15, no. 10, pp. 1783–1785, Jun. 2001, doi: 10.1096/fj.00-0820fje. Available: https://pubmed.ncbi.nlm.nih.gov/11481229/

16) N. E. Ward, N. R. Pellis, S. A. Risin, and D. Risin, "Gene Expression Alterations in Activated Human T-cells Induced by Modeled Microgravity," Journal of Cellular Biochemistry, vol. 99, no. 4, pp. 1187–1202, Jan. 2006, doi: 10.1002/jcb.20988. Available: https://pubmed.ncbi.nlm.nih.gov/16795038/

17) T. T. Chang et al., "The Rel/NF-κB Pathway and Transcription of Immediate Early Genes in T Cell Activation Are Inhibited by Microgravity," Journal of Leukocyte Biology, vol. 92, no. 6, pp. 1133–1145, Jul. 2012, doi: 10.1189/jlb.0312157. Available: https://pubmed.ncbi.nlm.nih.gov/22750545/

18) S. Tauber, S. Christoffel, C. S. Thiel, and O. Ullrich, "Transcriptional Homeostasis of Oxidative Stress-Related Pathways in Altered Gravity," International Journal of Molecular Sciences, vol. 19, no. 9, p. 2814, Sep. 2018, doi: 10.3390/ijms19092814. Available: https://pubmed.ncbi.nlm.nih.gov/30231541/

19) E. S. Baker, M. R. Barratt, C. F. Sams, and M. L. Wear, "Human Response to Space Flight," in Springer eBooks, 2019, pp. 367–411. doi: 10.1007/978-1-4939-9889-0_12. Available: https://doi.org/10.1007/978-1-4939-9889-0_12

20) S. Trappe et al., "Exercise in Space: Human Skeletal Muscle After 6 Months Aboard the International Space Station," Journal of Applied Physiology, vol. 106, no. 4, pp. 1159–1168, Jan. 2009, doi: 10.1152/japplphysiol.91578.2008. Available: https://doi.org/10.1152/japplphysiol.91578.2008

21) A. D. Moore, M. E. Downs, S. M. C. Lee, A. H. Feiveson, P. Knudsen, and L. Ploutz-Snyder, "Peak Exercise Oxygen Uptake During and Following Long-Duration

Spaceflight," Journal of Applied Physiology, vol. 117, no. 3, pp. 231–238, Jun. 2014, doi: 10.1152/japplphysiol.01251.2013. Available: https://doi.org/10.1152/japplphysiol.01251.2013

22) J. D. Sibonga, E. R. Spector, S. L. Johnston, and W. J. Tarver, "Evaluating Bone Loss in ISS Astronauts," Aerospace Medicine and Human Performance, vol. 86, no. 12:Supplement, pp. A38–A44, Nov. 2015, doi: 10.3357/amhp.ec06.2015. Available: https://pubmed.ncbi.nlm.nih.gov/26630194/

23) C. Richter, B. Braunstein, A. Winnard, M. Nasser, and T. Weber, "Human Biomechanical and Cardiopulmonary Responses to Partial Gravity – a systematic review," Frontiers in Physiology, vol. 8, Aug. 2017, doi: 10.3389/fphys.2017.00583. Available: https://doi.org/10.3389/fphys.2017.00583

24) NASA, "Apollo 15: Mission Details - NASA," NASA, Sep. 29, 2023. Available: https://www.nasa.gov/missions/apollo/apollo-15-mission-details/

25) C. Richter, B. Braunstein, A. Winnard, M. Nasser, and T. Weber, "Human Biomechanical and Cardiopulmonary Responses to Partial Gravity – a systematic review," Frontiers in Physiology, vol. 8, Aug. 2017, doi: 10.3389/fphys.2017.00583. Available: https://doi.org/10.3389/fphys.2017.00583

26) Apollo11Space, "Apollo Program Costs (New Data 1969 vs 2024)," Apollo11Space, Mar. 17, 2024. Available: https://apollo11space.com/apollo-program-costs-new-data-1969-vs-2024/

27) Apollo11Space, "Apollo Program Failures and Lessons Learned: NASA's Journey to the Moon," Apollo11Space, Aug. 18, 2024. Available: https://apollo11space.com/apollo-program-failures-and-lessons-learned-nasas-journey-to-the-moon/

28) F. E. Garrett-Bakelman et al., "The NASA Twins Study: A Multidimensional Analysis of a Year-Long Human Spaceflight," Science, vol. 364, no. 6436, Apr. 2019, doi: 10.1126/science.aau8650. Available: https://doi.org/10.1126/science.aau8650

29) "Twins Study - NASA," NASA. Available: https://www.nasa.gov/humans-in-space/twins-study/

30) S. Zhang, T. Adachi, S. Zhang, Y. Yoshida, and A. Takahashi, "A New Type of Simulated Partial Gravity Apparatus for Rats Based on a Pully-Spring System," Frontiers in Cell and Developmental Biology, vol. 10, Aug. 2022, doi: 10.3389/fcell.2022.965656. Available: https://pmc.ncbi.nlm.nih.gov/articles/PMC9472129/

31) M. Stephenson and W. Grayson, "Recent Advances in Bioreactors for Cell-Based Therapies," F1000Research, vol. 7, p. 517, Apr. 2018, doi: 10.12688/f1000research.12533.1. Available: https://pmc.ncbi.nlm.nih.gov/articles/PMC5931275/

32) "NASA Bioreactors Advance Disease Treatments | NASA Spinoff." Available: https://spinoff.nasa.gov/Spinoff2009/hm_3.html

33) J. Wong, "Cells in Space," Nature Medicine, vol. 3, no. 3, p. 259, Mar. 1997, doi: 10.1038/nm0397-259b. Available: https://www.nature.com/articles/nm0397-259b

34) The Editors of Encyclopaedia Britannica, "Physical Constant | Definition, Examples & Units," Encyclopedia Britannica, Jul. 20, 1998. Available: https://www.britannica.com/science/physical-constant

35) Hasenstein, K. H., & Van Loon, J. J. W. A. (2022). Clinostats and Other Rotating Systems—Design, Function, and Limitations. In River Publishers eBooks (pp. 147–156). https://doi.org/10.1201/9781003338277-17

36) "Zero Gravity Noun - Definition, Pictures, Pronunciation and Usage Notes | Oxford Advanced Learner's Dictionary at OxfordLearnersDictionaries.com." Available: https://www.oxfordlearnersdictionaries.com/definition/english/zero-gravity

37) Cook, A. H, Nordtvedt, K. L, Faller, and J. E, "Gravity | Definition, Physics, & Facts," Encyclopedia Britannica, Aug. 13, 2025. Available: https://www.britannica.com/science/gravity-physics/Newtons-law-of-gravity

38) J. Sánchez-Haro, I. Lombillo, and G. Capellán, "Simplified Model to Consider Influence of Gravity on Impacts on Structures: Experimental and Numerical Validation," International Journal of Impact Engineering, vol. 173, p. 104474, Dec. 2022, doi: 10.1016/j.ijimpeng.2022.104474. Available: https://www.sciencedirect.com/science/article/pii/S0734743X22003141

39) D. R. Morrison, ed., "Space Bioreactor Science Workshop", Johnson Space Center, Houston, TX; National Aeronautics and Space Administration, Washington, D.C., NASA CP-2485, Aug. 1985. Available: https://archive.org/download/Bioreactor01/bioreactor%2001.pdf.

40) NASA, "What is Microgravity? - NASA," NASA, Jul. 25, 2023. Available: https://www.nasa.gov/centers-and-facilities/glenn/what-is-microgravity/

41) A. Manzano et al., "Novel, Moon and Mars, Partial Gravity Simulation Paradigms and Their Effects on the Balance Between Cell Growth and Cell Proliferation During Early Plant Development," Npj Microgravity, vol. 4, no. 1, Mar. 2018, doi: 10.1038/s41526-018-0041-4. Available: https://www.nature.com/articles/s41526-018-0041-4

42) R. S. Thombre, K. Kaur, S. S. Jagtap, J. Dixit, and P. V. Vaishampayan, "Microbial Life in Space," in New Frontiers in Astrobiology, Elsevier, 2022, pp. 135–166. [Online]. Available: https://www.sciencedirect.com/science/article/abs/pii/B9780128241622000130

43) V. Chantseva, T. Bilova, G. Smolikova, A. Frolov, and S. Medvedev, "3D-Clinorotation Induces Specific Alterations in Metabolite Profiles of Germinating Brassica Napus L.

Seeds," Biological Communications, vol. 64, no. 1, pp. 55–74, Jan. 2019, doi: 10.21638/spbu03.2019.107. Available: https://www.researchgate.net/publication/333850184_3D-clinorotation_induces_specific_alterations_in_metabolite_profiles_of_germinating_Brassica_napus_L_seeds

44) F. J. Medina, A. Manzano, A. Villacampa, M. Ciska, and R. Herranz, "Understanding Reduced Gravity Effects on Early Plant Development Before Attempting Life-Support Farming in the Moon and Mars," Frontiers in Astronomy and Space Sciences, vol. 8, Sep. 2021, doi: 10.3389/fspas.2021.729154. Available: https://www.researchgate.net/publication/354358925_Understanding_Reduced_Gravity_Effects_on_Early_Plant_Development_Before_Attempting_Life-Support_Farming_in_the_Moon_and_Mars

45) B. R. Unsworth and P. I. Lelkes, "Growing Tissues in Microgravity," Nature Medicine, vol. 4, no. 8, pp. 901–907, Aug. 1998, doi: 10.1038/nm0898-901. Available: https://www.nature.com/articles/nm0898-901

46) "United Nations Sustainable Development Goals (SDGs)," UN Regional Information Centre for Western Europe, UNRIC. Available: https://unric.org/en/united-nations-sustainable-development-goals/

47) "Goal 3 | Good Health and Well-Being." Available: https://sdgs.un.org/goals/goal3

48) "Goal 12 | Responsible Consumption and Production." Available: https://sdgs.un.org/goals/goal12

49) F. Palladino et al., "Bioreactors: Applications and Innovations For A Sustainable And Healthy Future—A Critical Review," Applied Sciences, vol. 14, no. 20, p. 9346, Oct. 2024, doi: 10.3390/app14209346. Available: https://www.researchgate.net/publication/384925238_Bioreactors_Applications_and_Innovations_for_a_Sustainable_and_Healthy_Future-A_Critical_Review

50) "Goal 13 | Climate Action." Available: https://sdgs.un.org/goals/goal13

51) "Goal 9 | Industry, Innovation, and Infrastructure." Available: https://sdgs.un.org/goals/goal9

52) "FAQs : The International Space Station Transition Plan - NASA," NASA. Available: https://www.nasa.gov/faqs-the-international-space-station-transition-plan/#q3

53) "Destinations - NASA," NASA. Available: https://www.nasa.gov/humans-in-space/destinations/

54) J. Swanenburg, C. A. Easthope, A. Meinke, A. Langenfeld, D. A. Green, and P. Schweinhardt, "Lunar and Mars Gravity Induce Similar Changes in Spinal Motor Control as Microgravity," Frontiers in Physiology, vol. 14, Jul. 2023, doi:

10.3389/fphys.2023.1196929. Available: https://pmc.ncbi.nlm.nih.gov/articles/PMC10411353/

55) Harland and D. M, "Microgravity | Space Exploration, Astronauts & Zero-Gravity," Encyclopedia Britannica, Nov. 19, 2007. Available: https://www.britannica.com/science/microgravity

56) "Scientists Create Model to Measure How Cells Sense Their Surroundings," ScienceDaily, Mar. 20, 2020. Available: https://www.sciencedaily.com/releases/2020/03/200326144348.htm

57) "Gravity: It's Only a Theory | National Center for Science Education." Available: https://ncse.ngo/gravity-its-only-theory

58) J. Berro, "'Essentially, All Models Are Wrong, But Some Are Useful'—A Cross-Disciplinary Agenda for Building Useful Models in Cell Biology and Biophysics," Biophysical Reviews, vol. 10, no. 6, pp. 1637–1647, Nov. 2018, doi: 10.1007/s12551-018-0478-4. Available: https://pmc.ncbi.nlm.nih.gov/articles/PMC6297095/

59) Nuaire, "NU-5810 High Heat Decontamination CO2 incubator," www.nuaire.com. Available: https://www.nuaire.com/products/co2-incubators/direct-heat/in-vitrocell-nu-5810-direct-heat-decon-co2-incubator

60) C.-P. Segeritz and L. Vallier, "Cell Culture," in Elsevier eBooks, 2017, pp. 151–172. doi: 10.1016/b978-0-12-803077-6.00009-6. Available: https://www.sciencedirect.com/science/article/pii/B9780128030776000096

61) Standard Guide for Quantifying Cell Viability and Related Attributes within Biomaterial Scaffolds," ASTM F2739-19, ASTM International, 2019. Available: https://compass.astm.org/document/?contentCode=ASTM%7CF2739-19%7Cen-US&proxycl=https%3A%2F%2Fsecure.astm.org&fromLogin=true

62) A. Simonyan and N. Sarvazyan, "Bioreactors," in Learning materials in biosciences, 2020, pp. 127–136. doi: 10.1007/978-3-030-39698-5_11. Available: https://doi.org/10.1007/978-3-030-39698-5_11

63) M. Stephenson and W. Grayson, "Recent Advances in Bioreactors for Cell-Based Therapies," F1000Research, vol. 7, p. 517, Apr. 2018, doi: 10.12688/f1000research.12533.1. Available: https://pmc.ncbi.nlm.nih.gov/articles/PMC5931275/

64) Fern J. Armistead, Julia Gala De Pablo, Hermes Gadêlha, Sally A. Peyman, Stephen D. Evans, "Cells Under Stress: An Inertial-Shear Microfluidic Determination of Cell Behavior," Biophysical Journal, vol. 116, issue 6, pgs. 1127-1135, 2019, ISSN 0006 3495. Available: https://doi.org/10.1016/j.bpj.2019.01.034

65) C. A. Nickerson, C. M. Ott, J. W. Wilson, R. Ramamurthy, and D. L. Pierson, "Microbial Responses to Microgravity and Other Low-Shear Environments," Microbiology and

Molecular Biology Reviews, vol. 68, no. 2, pp. 345–361, Jun. 2004, doi: 10.1128/mmbr.68.2.345-361.2004. Available: https://pmc.ncbi.nlm.nih.gov/articles/PMC419922/

66) D. Nowacki, F. G. Klinger, G. Mazur, and M. De Felici, "Effect of Culture in Simulated Microgravity on the Development of Mouse Embryonic Testes," Advances in Clinical and Experimental Medicine, vol. 24, no. 5, pp. 769–774, Sep. 2015, doi: 10.17219/acem/27920. Available: https://www.researchgate.net/publication/283754366_Effect_of_Culture_in_Simulated_Microgravity_on_the_Development_of_Mouse_Embryonic_Testes

67) H. Andrade-Zaldívar, L. Santos, and A. De León Rodríguez, "Expansion of Human Hematopoietic Stem Cells for Transplantation: Trends and Perspectives," Cytotechnology, vol. 56, no. 3, pp. 151–160, Mar. 2008, doi: 10.1007/s10616-008-9144-1. Available: https://www.researchgate.net/publication/23467300_Expansion_of_human_hematopoietic_stem_cells_for_transplantation_Trends_and_perspectives

68) M. A. Phelan, A. L. Gianforcaro, J. A. Gerstenhaber, and P. I. Lelkes, "An Air Bubble-Isolating Rotating Wall Vessel Bioreactor for Improved Spheroid/Organoid Formation," Tissue Engineering Part C Methods, vol. 25, no. 8, pp. 479–488, Jul. 2019, doi: 10.1089/ten.tec.2019.0088. Available: https://pmc.ncbi.nlm.nih.gov/articles/PMC6686703/?term=%22Tissue%20Eng%20Part%20C%20Methods%22%5Bjour%5D

69) Phelan, M. A. (2018). The design, construction, and validation of novel rotating wall vessel bioreactors (Master's thesis, Temple University). Temple University Graduate Board.

70) Phelan, M. A. (2021). Bioengineering approaches for improved differentiation of cultured retinal tissues from pluripotent stem cells (Doctoral dissertation, Temple University). Temple University Graduate Board.

71) P. R. Cavanagh et al., "A Novel Lunar Bed Rest Analogue," Aviation Space and Environmental Medicine, vol. 84, no. 11, pp. 1191–1195, Oct. 2013, doi: 10.3357/asem.3472.2013. Available: https://pubmed.ncbi.nlm.nih.gov/24279234/

72) G. R. ClÃ©Ment, A. P. Bukley, and W. H. Paloski, "Artificial Gravity as a Countermeasure for Mitigating Physiological Deconditioning During Long-Duration Space Missions," Frontiers in Systems Neuroscience, vol. 9, Jun. 2015, doi: 10.3389/fnsys.2015.00092. Available: https://www.researchgate.net/publication/279728802_Artificial_gravity_as_a_countermeasure_for_mitigating_physiological_deconditioning_during_long-duration_space_missions

73) "Centripetal Acceleration | Physics." Available: https://courses.lumenlearning.com/suny-physics/chapter/6-2-centripetal-acceleration/

74) G. Clément, “International Roadmap for Artificial Gravity Research,” Npj Microgravity, vol. 3, no. 1, Nov. 2017, doi: 10.1038/s41526-017-0034-8. Available: https://www.nature.com/articles/s41526-017-0034-8

75) J. L. P. Pavón, S. H. Martín, C. G. Pinto, and B. M. Cordero, “Determination of Trihalomethanes in Water Samples: A Review,” Analytica Chimica Acta, vol. 629, no. 1–2, pp. 6–23, Sep. 2008, doi: 10.1016/j.aca.2008.09.042. Available: https://www.researchgate.net/publication/23402927_Determination_of_trihalomethanes_in_water_samples_A_review

76) A. W. Nienow, B. Isailovic, and T. A. Barrett, “Design and Performance of Single-Use, Stirred-Tank bioreactors,” Jan. 30, 2024. Available: https://www.bioprocessintl.com/single-use/design-and-performance-of-single-use-stirred-tank-bioreactors

77) M. Scholz, “Weighted Decision Matrix: A Tool for Pro-Level Prioritization,” airfocus, Jun. 26, 2025. Available: https://airfocus.com/blog/weighted-decision-matrix-prioritization/

78) “Parabolic flight - NASA,” NASA. Available: https://www.nasa.gov/mission/parabolic-flight/

79) J. J. W. A. Van Loon, “Centrifuges for Microgravity Simulation. The Reduced Gravity Paradigm,” Frontiers in Astronomy and Space Sciences, vol. 3, Jul. 2016, doi: 10.3389/fspas.2016.00021. Available: https://doi.org/10.3389/fspas.2016.00021

80) The Editors of Encyclopaedia Britannica, “Equivalence Principle | Gravitational, Acceleration & Time Dilation,” Encyclopedia Britannica, Jul. 20, 1998. Available: https://www.britannica.com/science/equivalence-principle

81) A. Barzegari and A. A. Saei, “An Update to Space Biomedical Research: Tissue Engineering in Microgravity Bioreactors.,” DOAJ (DOAJ: Directory of Open Access Journals), Jan. 2012, doi: 10.5681/bi.2012.003. Available: https://pmc.ncbi.nlm.nih.gov/articles/PMC3648913/

82) A. L. Radtke and M. M. Herbst-Kralovetz, “Culturing and Applications of Rotating Wall Vessel Bioreactor Derived 3D Epithelial Cell Models,” Journal of Visualized Experiments, no. 62, Apr. 2012, doi: 10.3791/3868. Available: https://pmc.ncbi.nlm.nih.gov/articles/PMC3567125/

83) J. P. Licata, K. H. Schwab, Y.-E. Har-El, J. A. Gerstenhaber, and P. I. Lelkes, “Bioreactor Technologies for Enhanced Organoid Culture,” International Journal of Molecular Sciences, vol. 24, no. 14, p. 11427, Jul. 2023, doi: 10.3390/ijms241411427. Available: https://www.researchgate.net/publication/372622186_Bioreactor_Technologies_for_Enhanced_Organoid_Culture

84) T. J. Goodwin, T. L. Prewett, D. A. Wolf, and G. F. Spaulding, “Reduced Shear Stress: A Major Component in the Ability of Mammalian Tissues to Form Three-Dimensional Assemblies in Simulated Microgravity,” Journal of Cellular Biochemistry, vol. 51, no. 3, pp. 301–311, Mar. 1993, doi: 10.1002/jcb.240510309. Available: https://pubmed.ncbi.nlm.nih.gov/8501132/

85) T. G. Hammond and J. M. Hammond, “Optimized Suspension Culture: the Rotating-Wall Vessel,” AJP Renal Physiology, vol. 281, no. 1, pp. F12–F25, Jul. 2001, doi: 10.1152/ajprenal.2001.281.1.f12. Available: https://doi.org/10.1152/ajprenal.2001.281.1.f12

86) S. Navran, “The Application of Low Shear Modeled Microgravity to 3-D cell Biology and Tissue Engineering,” Biotechnology Annual Review, pp. 275–296, Jan. 2008, doi: 10.1016/s1387-2656(08)00011-2. Available: https://pubmed.ncbi.nlm.nih.gov/18606368/

87) A. Wnorowski et al., “Effects of Spaceflight on Human Induced Pluripotent Stem Cell-Derived Cardiomyocyte Structure and Function,” Stem Cell Reports, vol. 13, no. 6, pp. 960–969, Nov. 2019, doi: 10.1016/j.stemcr.2019.10.006. Available: https://pubmed.ncbi.nlm.nih.gov/31708475/

88) P. M. Gershovich, J. G. Gershovich, A. P. Zhambalova, Yu. A. Romanov, and L. B. Buravkova, “Cytoskeletal Proteins and Stem Cell Markers Gene Expression in Human Bone Marrow Mesenchymal Stromal Cells After Different Periods of Simulated Microgravity,” Acta Astronautica, vol. 70, pp. 36–42, Sep. 2011, doi: 10.1016/j.actaastro.2011.07.028. Available: https://www.sciencedirect.com/science/article/abs/pii/S0094576511002402

89) N. Yamaguchi et al., “Microbial Monitoring of Crewed Habitats in Space—Current status and Future Perspectives,” Microbes and Environments, vol. 29, no. 3, pp. 250–260, Jan. 2014, doi: 10.1264/jsme2.me14031. Available: https://www.researchgate.net/publication/264867408_Microbial_Monitoring_of_Crewed_Habitats_in_Space-Current_Status_and_Future_Perspectives

90) F. Arias et al., “Mars Artificial Gravity Habitat with Centrifugation (MAGICIAN),” IEEE Aerospace Conference, pp. 1–17, Mar. 2024, doi: 10.1109/aero58975.2024.10521126. Available: https://www.researchgate.net/publication/380558478_Mars_Artificial_Gravity_Habitat_with_Centrifugation_MAGICIAN

91) Barnard, R. Walter, Maor, and Eli, “Trigonometry | Definition, Formulas, Ratios, & Identities,” Encyclopedia Britannica, Aug. 18, 2025. Available: https://www.britannica.com/science/trigonometry

92) TrueGeometry, “How to Calculate RPM from Angular Velocity In Context of RPM to Angular Velocity,” True Geometry’s Blog, Sep. 12, 2024. Available: https://blog.truegeometry.com/tutorials/education/b372e069150d103d6263046cc3742829/JSON_TO_ARTCL_How_to_Calculate_RPM_from_Angular_Velocity_in_context_of_rpm_to_an.html

93) A. J. Banko and J. K. Eaton, “Particle Dispersion and Preferential Concentration in Particle-Laden Turbulence,” in Elsevier eBooks, 2023, pp. 43–79. doi: 10.1016/b978-0-32-390133-8.00011-6. Available: https://www.sciencedirect.com/topics/physics-and-astronomy/settling-velocity

94) Gregersen and Erik, “Stokes’s Law | Definition, Formula, & Facts,” Encyclopedia Britannica, Jul. 20, 1998. Available: https://www.britannica.com/science/Stokess-law

95) S. Yao, C. Chang, K. Hai, H. Huang, and H. Li, “A Review of Experimental Studies on the Proppant Settling in Hydraulic Fractures,” Journal of Petroleum Science and Engineering, vol. 208, p. 109211, Jul. 2021, doi: 10.1016/j.petrol.2021.109211. Available: https://www.sciencedirect.com/topics/engineering/particle-reynolds-number

96) D. A. Charlebois and G. Balázsi, “Modeling Cell Population Dynamics,” In Silico Biology, vol. 13, no. 1–2, pp. 21–39, Dec. 2018, doi: 10.3233/isb-180470. Available: https://pmc.ncbi.nlm.nih.gov/articles/PMC6598210/

97) E. M. Martinez, M. C. Yoshida, T. L. T. Candelario, and M. Hughes-Fulford, “Spaceflight and Simulated Microgravity Cause a Significant Reduction of Key Gene Expression in Early T-Cell Activation,” AJP Regulatory Integrative and Comparative Physiology, vol. 308, no. 6, pp. R480–R488, Jan. 2015, doi: 10.1152/ajpregu.00449.2014. Available: https://www.researchgate.net/publication/270659952_Spaceflight_and_simulated_microgravity_cause_a_significant_reduction_of_key_gene_expression_in_early_T-cell_activation

98) L. R. Brewer and P. R. Bianco, “Laminar Flow Cells for Single-Molecule Studies of DNA-Protein Interactions,” Nature Methods, vol. 5, no. 6, pp. 517–525, May 2008, doi: 10.1038/nmeth.1217. Available: https://pmc.ncbi.nlm.nih.gov/articles/PMC7141782/

99) K. Yamamoto, Y. Shimogonya, R. Maeno, K. Kawabe, and J. Ando, “Endothelial Cells Differentially Sense Laminar and Disturbed Flows by Altering the Lipid Order of Their Plasma and Mitochondrial Membranes,” AJP Cell Physiology, vol. 325, no. 6, pp. C1532–C1544, Nov. 2023, doi: 10.1152/ajpcell.00393.2023. Available: https://pmc.ncbi.nlm.nih.gov/articles/PMC10861177/

100) V. Chatziravdeli, G. N. Katsaras, and G. I. Lambrou, “Gene Expression in Osteoblasts and Osteoclasts Under Microgravity Conditions: A Systematic review,” Current Genomics, vol. 20, no. 3, pp. 184–198, Apr. 2019, doi: 10.2174/1389202920666190422142053. Available: https://pmc.ncbi.nlm.nih.gov/articles/PMC6935951/

101) J. Braveboy-Wagner and P. I. Lelkes, “Impairment of 7F2 Osteoblast Function by Simulated Partial Gravity in a Random Positioning Machine,” Npj Microgravity, vol. 8, no. 1, Jun. 2022, doi: 10.1038/s41526-022-00202-x. Available: https://pubmed.ncbi.nlm.nih.gov/35672327/

102) J. L. Brown and C. T. Laurencin, “Bone Tissue Engineering,” in Biomaterials Science, 2020, pp. 1373–1388. doi: 10.1016/b978-0-12-816137-1.00085-4. Available: https://www.sciencedirect.com/topics/materials-science/osteoblast?utm_source=chatgpt.com

103) G. E. Neurohr and A. Amon, “Relevance and Regulation of Cell Density,” Trends in Cell Biology, vol. 30, no. 3, pp. 213–225, Jan. 2020, doi: 10.1016/j.tcb.2019.12.006. Available: https://pmc.ncbi.nlm.nih.gov/articles/PMC8777196/

104) L. E. Bourne and I. R. Orriss, “Isolation and Culture of Osteoblasts,” Methods in Molecular Biology, pp. 3–22, Jan. 2025, doi: 10.1007/978-1-0716-4306-8_1. Available: https://doi.org/10.1007/978-1-0716-4306-8_1

105) C. Poon, “Measuring The Density and Viscosity of Culture Media for Optimized Computational Fluid Dynamics Analysis of In Vitro Devices,” Journal of the Mechanical Behavior of Biomedical Materials/Journal of Mechanical Behavior of Biomedical Materials, vol. 126, p. 105024, Dec. 2021, doi: 10.1016/j.jmbbm.2021.105024. Available: https://www.sciencedirect.com/science/article/pii/S1751616121006500

106) “Autoclavable High Aspect Ratio Vessels (HARVs),” Synthecon. Available: https://www.synthecon.com/products-1/autoclavable-high-aspect-ratio-vessels-(harvs)

107) “Autoclavable Slow Turning Lateral Vessels (STLVs),” Synthecon. Available: https://www.synthecon.com/copy-of-products-1/autoclavable-slow-turning-lateral-vessels-(stlvs)

108) “Nema 34 Stepper Motor 6A 12Nm (1700 oz-in) 156mm Length for CNC Router Mill Lathe - Amazon.com.” Available: https://www.amazon.com/Stepper-Motor-156mm-Length-Router/dp/B077XHBTZ9/ref=sr_1_6?crid=2F3A89D9L8KGF&dib=eyJ2IjoiMSJ9.WZRYDLvK4iy4MKHDqzgzW-KZ6IJVCGcMttPGLyGloRxVI-hWDTjgj23dxENGK6kS_6KkN4LdexRzhC1pegA292-DXSPlAYE9292EP619gGTYOpxU9hSM3e7EZU9-IbYnXxfbJId8llashgRuPM1Ggm0OQYTWchZ-LYiSNOLWDLWJJ-kOjLLcmHdTPVW5BLAAu_ddyR9XQ1nPmBNeMx528-HHRVKVBx-ig7xm9S6lLgCYzmpDSKRywcWsEUNU2YYEXrzCsyFQ61khWZggzf7FnJmt-ICqUBp7dosA9lhibBI.XjjzqFOeXWNvEjbFXi3V7hggREwal_kKYLPu-iNrG-w&dib_tag=se&keywords=nema+34&qid=1758432023&s=industrial&sprefix=nema+34+%2Cindustrial%2C58&sr=1-6

109) “CNC DSP Digital Microstep driver DM860H Stepper Motor Controller 2-phase Digital Stepper Motor Driver for Nema 23 Nema 34 series stepper motor, Replace DMA860H - Amazon.com.” Available: https://www.amazon.com/Digital-Microstep-Stepper-Controller-2-phase/dp/B08R3W93W3/ref=asc_df_B08R3W93W3?tag=bingshoppinga-20&linkCode=df0&hvadid=80333178202706&hvnetw=o&hvqmt=e&hvbmt=be&hvdev=c&hvlocint=&hvlocphy=94510&hvtargid=pla-4583932711718096&psc=1

110) Arduino, “Arduino Nano Every with Headers,” Arduino Online Store, 2025. Available: https://store-usa.arduino.cc/collections/nano-family/products/nano-every-with-headers

8. Supplementary Data

Supplementary Table S 1: Bioreactor Systems for Cell Expansion

Bioreactor type	Commercial examples	Parameter ranges	Advantages/limitations	Example case studies	References
Rocking bed (wave motion)	• WAVE (GE Healthcare) • Finesse (Thermo Fisher) • Biostat (Sartorius)	• Size (1–500 L) • Rocking angle: 5–35° • Rotation speed: 10–35 rpm	Advantages: • Versatile single-use bags Limitations: • Limited scale-up potential	• Cell type: hMSCs • Method: microcarrier culture • Culture time: 7 days • Fold expansion: 0.7–14.5 • Metrics: viability, tri-lineage differentiation, aggregate size	[1]
Stirred tank	• Mobius (EMD Millipore) • Finesse (Thermo Fisher)	• Size (100 mL–1,000 L) • Impeller power/speed: variable during culture period • Impeller design: updraft or downdraft, single or multiple	Advantages: • Functional at-large volumes: >50 L Limitations: • Shear forces may impact cell viability/differentiation	• Cell type: hMSCs, hASCs, hiPSCs, and murine ovary cell cells • Method: aggregates, microcarriers, and single-cell suspensions • Culture time: 11–17 days • Fold expansion: 25.7–43 • Metrics: viability, aggregate size, and differentiation capacity	[3][4][5][6]
Rotating wall vessels	RCCMAX (Synthecon)	• Size (100 mL–10 L) • Rotational speed: 5–20 rpm • Continuous medium recirculation or	Advantages: • Low turbulence • Can simulate microgravity Limitations: • Effective only at small volumes: <10 L	• Cell type: hMSCs • Method: scaffolds • Culture time: 21 days • Fold expansion: ~39	[7]

Bioreactor type	Commercial examples	Parameter ranges	Advantages/limitations	Example case studies	References
		closed batch system		• Metrics: viability, surface marker expression, and differentiation	
Perfusion bioreactor	• FiberCell (FiberCell Systems) • Quantum Cell Expansion (Terumo BCT)	• Size (100 mL–5 L) • Perfusion: direct (for example, through scaffolds) or indirect (hollow-fiber, encapsulated cells)	Advantages: • Limited turbulence • Can be automated • Compact Limitations: • Shear forces may impact cell viability/differentiation	• Cell type: hMSCs • Method: encapsulation • Culture time: 21 days • Fold expansion: not applicable • Metrics: viability and differentiation	[8][9]
Isolation/expansion automated systems	• G-Rex (Wilson Wolf) • CliniMACs Prodigy (Miltenyi Biotec)	• Size (100 mL) • Degree of automation	Advantages: • Versatile single-use bags • Automated cell isolation, manipulation, and expansion • GMP-compliant Limitations: • Primarily T-cell expansion	• Cell type: human lymphocytes • Method: suspension culture • Culture time: 8–14 days • Fold expansion: 32–63 • Metrics: viability and cell marker evaluation	[10][11]

GMP, good manufacturing practices; hASC, human adipose-derived stem cell; hiPSC, human induced pluripotent stem cell; hMSC, human mesenchymal stem cell.

Supplementary Table S 1 shows a summary of the different types of bioreactors for cell expansion. It includes their commercial examples, parameter ranges, advantages/ limitations, and example case studies [2].

Supplementary Code S 1. Starter Code

The code is found in the following zip file:
https://1drv.ms/u/c/e85d9878566ceed3/ER5cWSmWmpJDrhd9jn7kGKUBCelUvRZqTDHELMlEzzOmug?e=xYZXKU

9. Supplementary Data References

1) A. Shekaran et al., “Biodegradable ECM-coated PCL Microcarriers Support Scalable Human Early MSC Expansion and In Vivo Bone Formation,” Cytotherapy, vol. 18, no. 10, pp. 1332–1344, Aug. 2016, doi: 10.1016/j.jcyt.2016.06.016. Available: https://pubmed.ncbi.nlm.nih.gov/27503763/

2) M. Stephenson and W. Grayson, “Recent Advances in Bioreactors for Cell-Based Therapies,” F1000Research, vol. 7, p. 517, Apr. 2018, doi: 10.12688/f1000research.12533.1. Available: https://pmc.ncbi.nlm.nih.gov/articles/PMC5931275/

3) Tanja A. Grein, Jasmin Leber, Miriam Blumenstock, Florian Petry, Tobias Weidner, Denise Salzig, Peter Czermak, "Multiphase Mixing Characteristics in a Microcarrier-Based Stirred Tank Bioreactor Suitable for Human Mesenchymal Stem Cell Expansion", Process Biochemistry,vol. 51, issue 9,pgs 1109-1119,2016,ISSN 1359-5113. Available: https://doi.org/10.1016/j.procbio.2016.05.010

4) D. C. Surrao et al., “Large-Scale Expansion of Human Skin-Derived Precursor Cells (hSKPs) in Stirred Suspension Bioreactors,” Biotechnology and Bioengineering, vol. 113, no. 12, pp. 2725–2738, Jun. 2016, doi: 10.1002/bit.26040. Available: https://pubmed.ncbi.nlm.nih.gov/27345530/

5) T. Lawson et al., “Process Development for Expansion of Human Mesenchymal Stromal Cells in a 50L Single-Use Stirred Tank Bioreactor,” Biochemical Engineering Journal, vol. 120, pp. 49–62, Nov. 2016, doi: 10.1016/j.bej.2016.11.020. Available: https://www.sciencedirect.com/science/article/pii/S1369703X16303266

6) S. Markert and K. Joeris, “Establishment of a Fully Automated Microtiter Plate-Based System for Suspension Cell Culture and its Application for Enhanced Process Optimization,” Biotechnology and Bioengineering, vol. 114, no. 1, pp. 113–121, Jul. 2016, doi: 10.1002/bit.26044. Available: https://pubmed.ncbi.nlm.nih.gov/27399304/

7) M. C. Varley, A. E. Markaki, and R. A. Brooks, “Effect of rotation on scaffold motion and cell growth in rotating bioreactors,” Tissue Engineering Part A, vol. 23, no. 11–12, pp. 522–534, Jan. 2017, doi: 10.1089/ten.tea.2016.0357. Available: https://pubmed.ncbi.nlm.nih.gov/28125920/

8) B. B. Nguyen, H. Ko, and J. P. Fisher, “Tunable Osteogenic Differentiation of hMPCs in Tubular Perfusion System Bioreactor,” Biotechnology and Bioengineering, vol. 113, no. 8, pp. 1805–1813, Jan. 2016, doi: 10.1002/bit.25929. Available: https://pubmed.ncbi.nlm.nih.gov/26724678/

9) O. Ball, B.-N. B. Nguyen, J. K. Placone, and J. P. Fisher, “3D printed vascular networks enhance viability in High-Volume perfusion bioreactor,” Annals of Biomedical

Engineering, vol. 44, no. 12, pp. 3435–3445, Jun. 2016, doi: 10.1007/s10439-016-1662-y. Available: https://pubmed.ncbi.nlm.nih.gov/27272210/

10) U. Mock et al., "Automated Manufacturing of Chimeric Antigen Receptor T Cells for Adoptive Immunotherapy Using CliniMACS Prodigy," Cytotherapy, vol. 18, no. 8, pp. 1002–1011, Jul. 2016, doi: 10.1016/j.jcyt.2016.05.009. Available: https://pubmed.ncbi.nlm.nih.gov/27378344/

11) C. Priesner et al., "Automated Enrichment, Transduction, and Expansion of Clinical-Scale CD62L+ T cells for Manufacturing of Gene Therapy Medicinal Products," Human Gene Therapy, vol. 27, no. 10, pp. 860–869, Aug. 2016, doi: 10.1089/hum.2016.091. Available: https://pubmed.ncbi.nlm.nih.gov/27562135/